ZHANG, TIAN, Ph.D. Nanoparticle Toxicity in *Drosophila Melanogaster*: A Case Study with Nickel, Nickel Oxide, and Iron-Nickel Alloy Nanoparticles. (2018)
Directed by Dr. Amy Adamson. 105 pp.

With an increase use of nanomaterials, growing concerns have risen about their potential exposure to environment and the risk of side effects on human health. My research investigates the ecological and mechanistic insights of *in vivo* nanoparticle toxicology via oral exposure, specifically metallic nickel, nickel-iron alloy, and nickel oxide particles, using the *Drosophila melanogaste*r model system. In order to understand the physical and chemical behavior of the nickel-based nanoparticles that were used in this study, I characterized the particle size, morphology, aqueous aggregation state, and hydrodynamic zeta potential of these nanomaterials. I found that these nanomaterials displayed a distinct set of physicochemical properties and that these properties appear to have a significant role in the toxicological effects that I observed. Metallic nickel nanoparticles were toxic to the larvae *D. melanogaster*, having a dose-dependent mortality, a development delay in pupariation, inhibition of tissue growth, reduction of wing size, as well as the induction of the stress protein Hsp70 and ROS production. I also found unique fluorescent mineral depositions form in the Malpighian tubules after oral exposure to nickel nanoparticles. Energy-dispersive X-ray spectroscopy reveals that the chemical composition of these mineral crystals was calcium carbonate. The experimental evidence of the toxic effects of nickel nanoparticle effect via the oral route provides valuable information of risk and biohazard to the community.

NANOPARTICLE TOXICITY IN *DROSOPHILA MELANOGASTER:* A CASE STUDY WITH NICKEL, NICKEL OXIDE, AND IRON-NICKEL ALLOY NANOPARTICLES

by

Tian Zhang

A Dissertation Submitted to
the Faculty of The Graduate School at
The University of North Carolina at Greensboro
in Partial Fulfillment
of the Requirements for the Degree
Doctor of Philosophy

Greensboro
2018

Approved by

_____
Committee Chair

APPROVAL PAGE

This dissertation written by TIAN ZHANG has been approved by the following committee of the Faculty of The Graduate School at The University of North Carolina at Greensboro.

Committee Chair_____

Committee Members_____

_____

_____

_____

_____
Date of Acceptance by Committee

_____
Date of Final Oral Examination

TABLE OF CONTENTS

LIST OF TABLES

Page

LIST OF FIGURES

Page

CHAPTER I

INTRODUCTION

Nanoparticles are defined as objects with at least one dimension smaller than 100 nm, which exist either naturally or in manufactured forms (Oberdorster et al., 2005). Nanoparticles typically have large surface area to volume ratios and sometimes distinct physicochemical properties compared to the same substance in bulk. For example, nanogold exhibits a red color whereas bulk gold presents a yellow color (Faraday, 1857). This property of gold nanoparticles has been used for centuries as many of the red-stained glass used in churches throughout Europe is made with these materials (Schaming and Remita, 2015).

With an increase in the application of nanomaterials in the fields of biomedicine, electronics, consumer products, and many other aspects in industry and agriculture, the potential exposure of the environment to engineered nanoparticles raises concerns about the risk of side effects on human health. Between 2005 and 2015, the number of products containing nanoparticles increased dramatically by 30-fold, in 32 countries (Vance et al., 2015). In 2015, based on the inventory of nanoproducts on the market, there were more than 1800 products containing nanoparticles and 39 different types of nanomaterials (Nanotechnologies., 2015). Currently, nanotechnology is widely used in many industrial sectors, including medicine, energy, materials science, instrumentation, and consumer products and the expectation is that there will be continual and rapid growth in the use of

nanomaterial in the near future (Veruscka et al., 2017). Supporting this notion, global consumption of nanomaterials is estimated to be 584, 984 metric tons in 2018 with a compound annual growth rate of 21.1% for the period of 2014 to 2019 (McWilliams, 2014). While contributing to the global economy, nanotechnology also has been shown to disrupt the environment and human health (Bundschuh et al., 2018). Therefore, there is a compelling need to establish the risk assessment of nanomaterials.

Risk assessment is a systematic process to evaluate the potential risks after exposure to hazardous substances. Standard risk assessment involves selection of an appropriate adverse biological response to materials, determination of critical dose, calculation of equivalent human dose, and determination of lifetime concentrations with relative dose (Kuempel et al., 2006). However, very few risk assessments of nanomaterials have been conducted due to limited data. Additionally, not enough attention to nanomaterials' risk assessments has been drawn to public and government agencies, which makes it difficult to establish an official comprehensive protocol for safety management of nanomaterials. As the first governing body to develop nano-regulations, the European Union (EU) assumed that the development and innovations of nanomaterials are controllable and biocompatible. However, some are skeptical that the EU focus on safety considerations may endanger the nanotechnology development (Rodríguez, 2018). Taking into consideration all of the above limitations, when standard risk assessments of nanotechnology are not available, data from animals or cell systems are needed to determine the underlying mechanisms of nanotoxicity.

I selected the model genetic organism the fruit fly, *Drosophila melanogaste*r, as an *in vivo* model system for the toxicity evaluations of nickel (Ni), iron-nickel alloy (NiFe), and nickel oxide (NiO) nanoparticles. With a genome that contains homologues of genes involved with many human diseases, *Drosophila melanogaster* is an outstanding model system for the study of cancer, infectious disease, and neurological disorders (McLaughlin and Bratu, 2015). Furthermore, at the cellular and tissue level, both adult and larval Drosophila melanogaster have similar physiology and morphologies to human structures including a striking similarity with human gastrointestinal tract (Lemaitre and Miguel-Aliaga, 2013). For toxicological studies, the fruit fly is extremely convenient both as a model for effects on humans as well as effects on insects within an environment, as it has well characterized and relatively short life cycle and it is easy to manipulate and cultivate. Most interestingly, the food responses of Drosophila melanogaster provide a fantastic opportunity to study the ingestion toxicity of a nanomaterial considering that Drosophila larvae display rapid food intake and distinct developmental stages, which allow us to observe subtle effects from nanoparticle ingestion on development (Pandey and Nichols, 2011).

Among all possible exposure routes, the oral exposure route is highly relevant to human health as many applications of engineered nanoparticles have the potential for direct or indirect ingestion risks. A person may consume foods that are contaminated by nanoparticles during the preparation or packing processes (Amini et al., 2014), or ingest nanoparticles that have bio-accumulated in the food chain (Petersen and Henry, 2012). For example, although silica nanoparticles have been widely used as food additives in the

United States; it was until recently that silica nanoparticles arrest the cell cycle of human gastrointestinal cells at high dosages and therefore can be considered a potential hazard (Yang et al., 2014). Also, silica nanotubes are gaining great attention as efficient oral drug delivery carriers. Concerns for biomedical applications exist as inflammation by carbon-based nanotubes in the lungs have been shown in both *in vivo* and *in vitro* studies (Bergin and Witzmann, 2013). Moreover, there is evidence that nanoparticles can be absorbed in the gastrointestinal tract via the mucociliary escalator during inhalation exposure (Oberdörster et al., 2005).

The ease and simplicity of the delivery of nanomaterials via the oral route have made nanomaterials an attractive proposed vehicle for drugs and other therapeutics (Chow and Ho, 2013). Once in an organism, the unique chemical and physical properties of nanoparticles facilitate their entry into cells. Quantum dot nanoparticles were recognized, taken up by human epidermal keratinocytes and then translocated to lysosomes (Zhang and Monteiro-Riviere, 2009). As drug delivery vehicles, gold nanoparticles were also shown to be internalized in live cells through endocytosis (Yang et al., 2005). However, even in benign and beneficial applications, the impact that nanomaterials have on tissues in the alimentary canal are poorly understood, further emphasizing the urgent need for further investigations on oral exposure of nanoparticles.

Nickel and nickel compound nanoparticles have been gaining increasing attention due to their novel characteristics such as high surface energy, high magnetism, low melting point, and low burning point (Ahamed, 2011). For instance, nickel compounds are used as catalysts for synthesizing carbon nanotubes (Doustan and Pasha, 2016).

Researchers are optimizing nickel nanoparticles for drug delivery system in therapeutics (Prijic and Sersa, 2011). Green and novel synthesis of nickel nanoparticles are also constantly being improved (Wu et al., 2010). However, nickel-based nanoparticles have been shown to exhibit biological effect both *in vitro* and *in vivo*. After functionalization with a positive charge on the surface, nickel nanoparticles show increased uptake by hepatocellular carcinoma cells (Guo et al., 2009). Intravenous injection of nickel nanoparticles induces genotoxicity in rats (Magaye et al., 2012).

The goal of my dissertation research is to develop ecological and mechanistic insights into the *in vivo* nanotoxicology of nanoparticle ingestion, specifically metallic nickel, nickel-iron alloy, and nickel oxide particles, using the *Drosophila melanogaste*r model system. A detailed understanding of the developmental defects and underlying toxic mechanisms of these commonly used nanomaterials will contribute to current risk assessment of nanoparticles specific to nickel nano-materials, but also potentially to all metal and metal oxide nanomaterials. My study will direct more attention to the importance of nano-toxicity of new and emerging nanomaterials and also provide a methodology to the process of studying the toxicology of nanomaterials using the *Drosophila melanogaster* model system. Currently, there is a rapid expansion of the application of new and novel nanomaterials in a huge range of consumer goods and industrial application, but the impact of the materials, as well as the methods to determine risk and to characterize this risk, have not been developed at a similar pace. I have identified the toxic impacts of nickel metal and metal oxide nanoparticles via the oral route in a complex eukaryotic model system, *Drosophila melanogaster*, showing

increased mortality in a dose-dependent manner. Our study also provides important information regarding the oral exposure model and presents the advantages of using fruit flies as *in vivo* model for nanoparticle toxicity.

My evaluation of the toxic effects of metallic and metal oxide nanoparticle effect via the oral route provides valuable information of risk and biohazard to the community, from the perspectives of both human and environmental health. My project is innovative as the first *in vivo* study to test ingestion of different metallic and metal oxide nanoparticles using the *Drosophila* model system. My research is the first to present the deleterious effects of nickel nanoparticle ingestion. Another innovation of my project is to link heavy metal detoxification to nanoparticle ingestion by the formation of mineral crystals in the Malpighian tubule. I also propose a mechanism for the observed toxicity that involves connections of Hypoxia-inducible factor -1α, MT activation, heat shock protein-70 and oxidative stress pathways that are induced by nickel nanoparticles in.

CHAPTER II

LITERATURE REVIEW

2.1 Different Types of Nanoparticles

There are many different types of nanoparticles with distinct compositions and functionalities for use in applications such as catalysts, drug delivery, and as additives to consumer products (Dhand et al., 2015). For example, silver nanoparticles have been applied to textiles in medical environments due to their antimicrobial properties (Ballottin et al., 2017). Dendrimers, organic polymeric nanoparticles, are used as drug carriers for chemotherapeutic agent delivery (Medina and El-Sayed, 2009). Titanium dioxide nanoparticles have been used in water purification as a photocatalyst for hydrogen production (Ni et al., 2007)The properties of nanoparticles are dependent on their size, chemical composition, coating, and surface charge (Sukhanova et al., 2018). It is through these parameters that the desired properties are built into the nanoparticles. A great example of this is cadmium selenide quantum dot, whose optical fluorescent properties can be tuned in a size-dependent fashion (Jovin, 2003). In table 1, I highlight the major characteristics and uses of several common nanoparticles.

Table 1. Major Characteristics of Common Nanomaterials.

Types of nanoparticles	Remark properties	Application (Examples)	Concerns	References
Metal-based nanoparticles	Optical, electrical	Antimicrobial agents; Catalysts; Semiconductor; Drug delivery	Element-specific toxicity; Oxidative stress	(Bhattacharya and Mukherjee, 2008; Mody et al., 2010)
Fullerenes	Radical scavenging	Anti-aging cosmetic products	Immunotoxicity	(Benn et al., 2011; Lin and Lu, 2012)
Quantum dots	Photocatalytic	Semiconductor	Metabolism	(Jovin, 2003; Libralato et al., 2017)
Polystyrene nanoparticles	Biocompatible, hardly degradable	Fluorescent probes; Drug delivery	Unknown	(Loos et al., 2014)
Dendrimer	Monodispersing highly branched 3-dimensional architecture	Drug carriers; Tissue engineering; Transfection; MRI	Cytotoxic for cationic functional groups; Metabolic path	(Mintzer and Grinstaff, 2011)
Liposome	Completely biodegradable, hydrophilic/ hydrophobic	Administration of nutrients; Pharmaceutical drugs	Hypersensitivity reactions; Fewer stables	(Akbarzadeh et al., 2013)
Carbon nanotubes	Thermal conductivity, mechanical, electrical	Baseball bats; Car parts	Inflammatory responses	(De Volder et al., 2013; Liu et al., 2013)

2.1.1 Metallic Nanoparticles

Metallic nanoparticles are defined as nanoscale metals, either crystalline or amorphous, with at least one dimension (length, width, or thickness) is within the range of 1-100 nm. In 1857, Michael Faraday recognized the existence of metallic nanoparticles in the ruby colored colloidal gold and initiated the first investigations into the relationship between optical properties and metal particles (Faraday, 1857). Since then optical effects have been discovered in other metallic nanoparticles; silver nanoparticles exhibit a brilliant yellow color compared to bulk or ionic silver (Mulfinger et al., 2007). In addition to their interesting optical properties, metallic nanoparticles also possess unique electronic and magnetic properties. For instance, titanium dioxide nanoparticle-covered electrodes have altered electrochemical properties and enhanced conductivity as compared to traditional electrodes with the same composition (Loberg et al., 2013). Zinc ferrite nanoparticles have much higher magnetization than bulk forms have (Nunes et al., 1983). The fascinating properties of metallic nanoparticles are mainly the result of an exaggerated surface area–to–volume ratio when compared to the corresponding bulk metallic materials and make them attractive materials for a wide range of applications. Since the late 1990's , the number of publications that are focused on metallic nanoparticle been grown exponentially (Campelo et al., 2009). During 1992 – 2017, a total of 618,122 publications were identified by searching with 'metal nanoparticles' in the range of all fields, and a total of 71,123 publications were also available with the same search in the range of keywords on Scopus (www-Scopus-com.). The dramatically increasing trends over the years are shown in Figure 1.

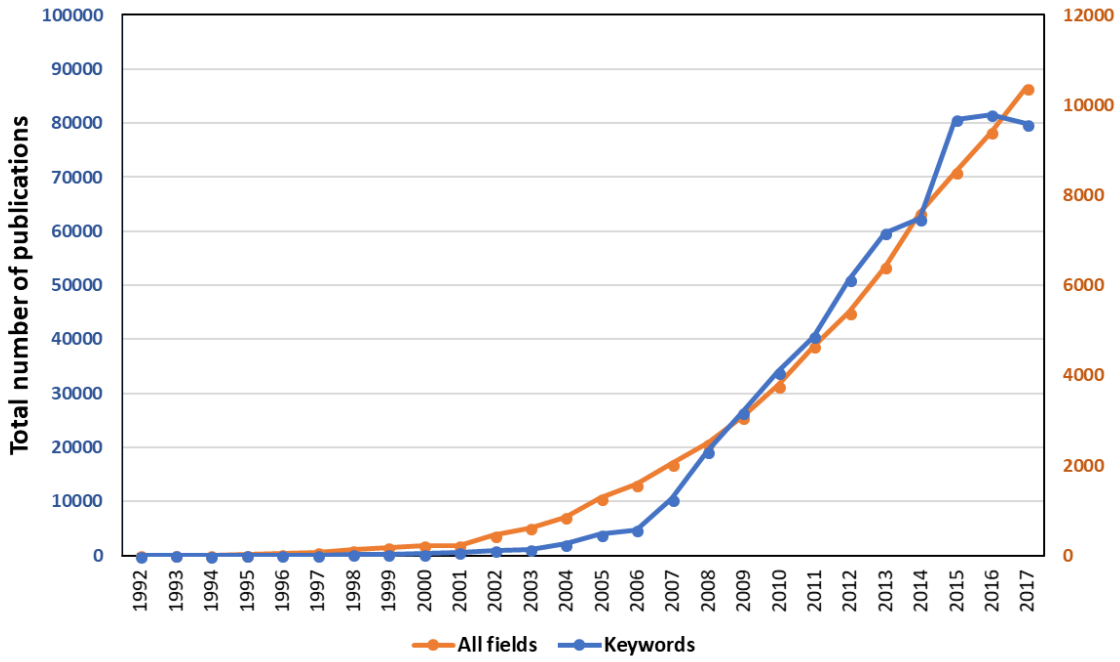

Figure 1. The Increase of Publications when Queried with ‘Metal Nanoparticles’ per Year. Each data plot shows the number of research articles containing “metal nanoparticles” within the range of ‘All field’ (Orange) or the range of ‘Keywords’ in database Scopus between 1992 and 2017.

2.1.1.1 Synthesis of Metallic Nanoparticles

Metallic nanoparticles are generated by either a top-down approach or a bottom-up approach (Figure 2). In a top-down approach, fabrications begin with the solid state of bulk materials and then reduction to the nanoscale. Top-down productions induce physical processing methods such as mechanical etching/milling/grinding and as well as traditional lithographic techniques (Wang et al., 2004). The illustrations of various top-down nanotechnology approaches are shown in Figure 3.

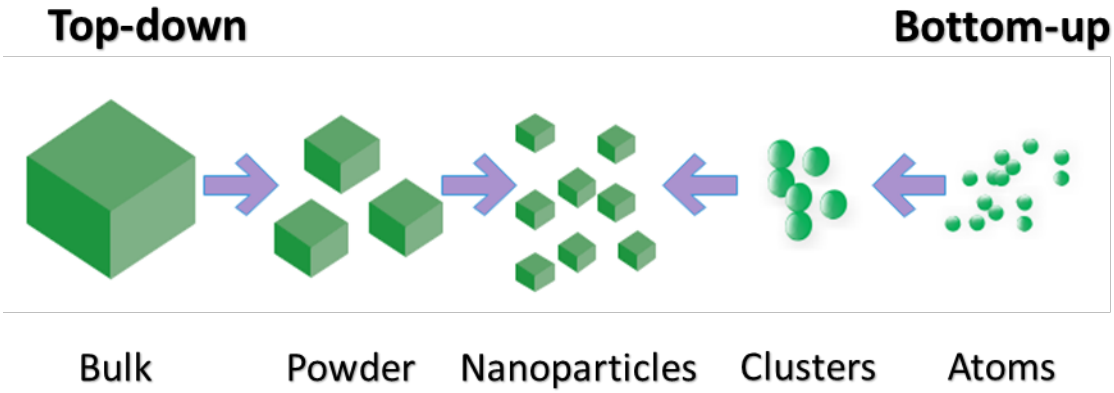

Figure 2. Schematic Diagram of Top-Down and Bottom-Up Approaches for Nanoparticle Synthesis. Top-down approaches refer to slicing cut the bulk material to smaller size to get nanoparticles. Bottom-up approaches refer to build up nanoparticles from atoms.

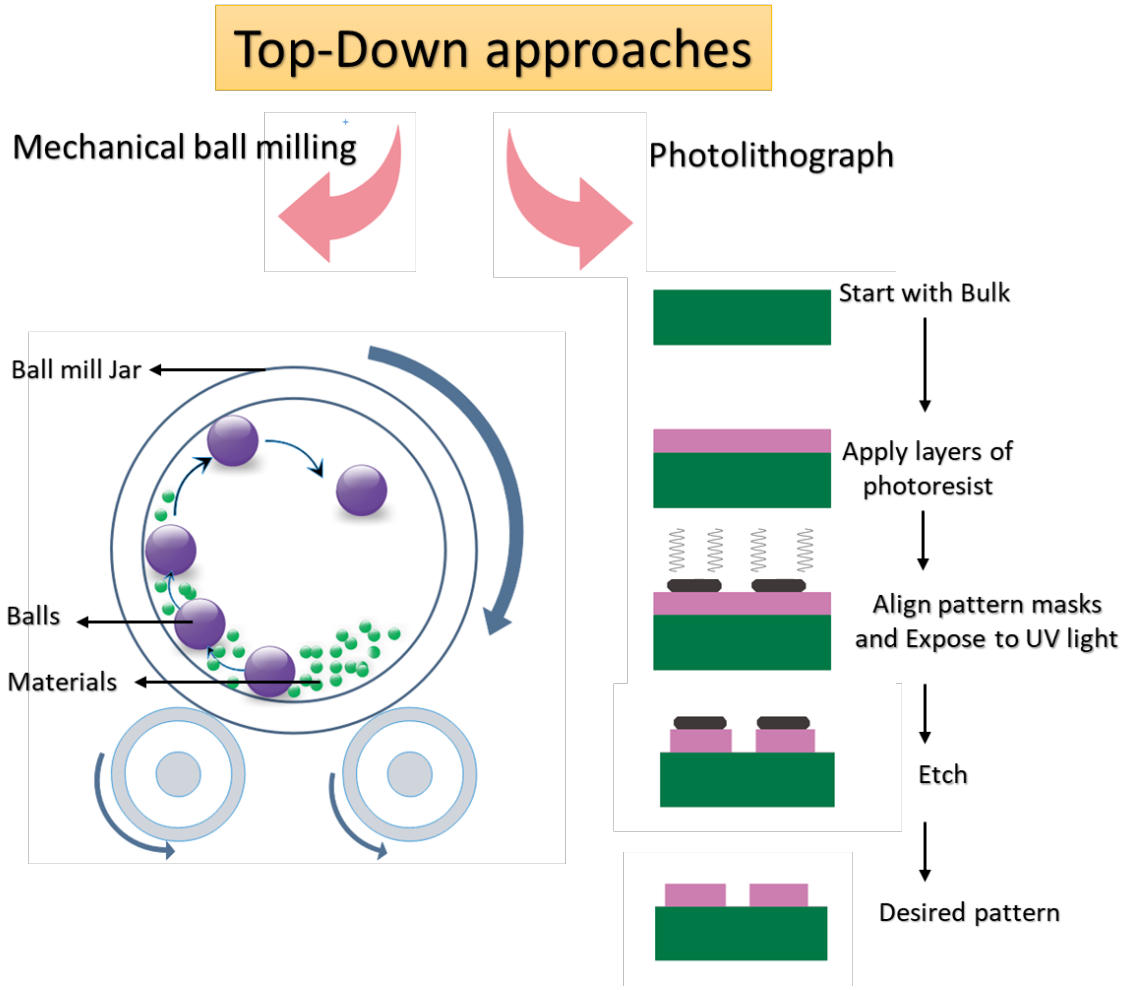

Figure 3. Schematic Diagram of Two Common Top-Down Approaches for Nanoparticle Preparation: Mechanical Ball Milling and General Lithograph. A mechanical ball mill is equipped with a cylindrical device loaded with bulk materials and milling balls. High-energy collisions from milling balls crush the bulk materials into nanoparticles during rotation. Photolithograph method requires deposition of photo-resistant layer coating and specific pattern on the wafer surface. Then short wavelength light etches the materials to produce sub 100-nm patterns.

In a bottom-up approach, the starting material is either in the gaseous state or liquid state which is then built up into nanoparticles (Mittal et al., 2013). Bottom-up syntheses include evaporation, sputtering, plasma, sol-gel, and solvothermal methods (Capek, 2017).

Although there are a number of different synthesis methods available to generate metallic nanoparticles today, only a few processes are used for large-scale production. Additionally, top-down methods usually exhibit imperfections of the nanoparticles surface structure of the nanoparticle and non-uniform size distributions, which is not desirable for many industrial applications. Currently, bottom-up liquid-phase synthetic processes account for a majority of the large-scale synthesis of commercial products (Charitidis et al., 2014). The general principle of a liquid phase synthesis is the reduction of dilute solutions of metal salts, a general scheme of the liquid-phase synthetic process is shown in Figure 4A. The major reason for using liquid-phase methods is that metallic nanoparticle preparation methods need to be reliable, reproducible and enable the controlled generations of particles of specific sizes, shapes and aggregation/dispersions. Another commonly used method in manufacture of making metallic nanoparticles is electrical wire explosion, whose production rate can reach 100g/hour (Kurlyandskaya et al., 2011; Pareek et al., 2017). This method utilizes a high voltage to evaporate the metallic materials between anode and cathode for the fabrication of nanoparticles (Figure 4B).

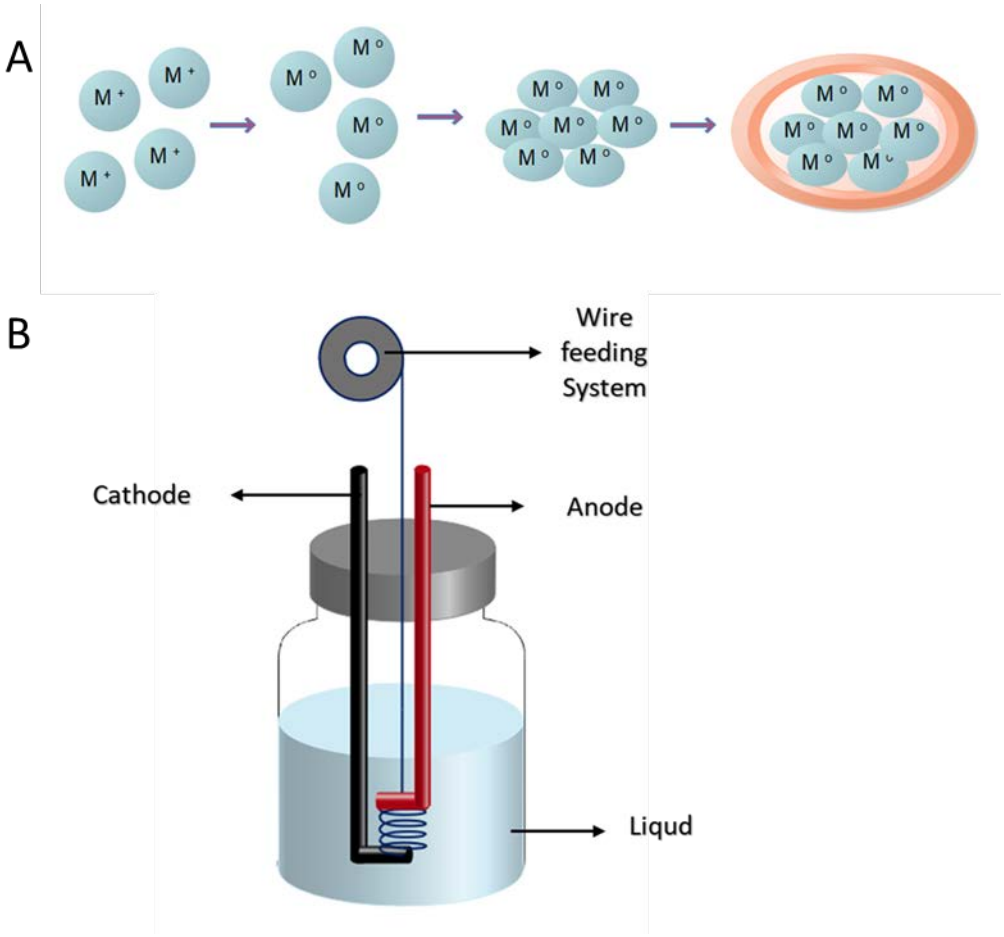

Figure 4. Schematic Illustrations of Bottom-Up Nanofabrication of Metallic Nanoparticles. A) The chemical reducing process involves reduction of metal salt solution with appropriate reducing agents and followed by stabilizing nanoparticles with capping agents. B) High voltage produces a high-density current pulse which passes through the pure (>99.9%) metallic wire. The thin wire is evaporated then immediately cooled and coated by surrounding agents.

All current commercially relevant synthetic processes, both chemical and physical methods, generate large amounts of waste materials and use toxic reagents (Raveendran et al., 2003). Recently there has been a drive for the use of the environmentally friendly methods of metallic nanoparticle syntheses that use less toxic precursors such as plant extracts or agricultural waste material (Mohamed et al., 2018). Chevva and Chandran et al. have reported a chitosan-based synthetic method to make silver nanowires as an eco-friendly approach. However, many of these "green" environmentally friendly processes are less efficient in yield and quality of the metallic nanoparticles. Therefore, a continuing trend in this type of research is the development of new and novel green synthetic strategies using renewable materials with higher yields and more uniform nanoparticles.

2.1.1.2 Application of Metallic Nanoparticles

Metallic nanoparticles have been applied in various fields depending on their individual properties. Some of the metallic nanoparticles, such as silver, gold, and copper nanoparticles, have received great attention for their antimicrobial activity (Dizaj et al., 2014). Gold nanoparticles are often used in biological delivery and imaging (Cabuzu et al., 2015). Nickel nanoparticles have been shown to have marked catalytic activity (Morozov et al., 2011). Iron nanoparticles are applied in magnet data storage, resonance imaging, and catalysts (Zhang, 2003).

2.1.2 Metal-Oxide Nanoparticles

Metal-oxide nanoparticles are produced using two strategies: liquid-solid approaches and gas-solid approaches (Tuli et al., 2015). Metal oxides have many interesting and useful chemical properties such as redox potential, catalytic effects, mechanical and chemical stability, and biocompatibility. Nanoparticles of silver oxide (Ag_2O), titanium dioxide (TiO_2), zinc oxide (ZnO), calcium oxide (CaO), and magnesium oxide (MgO) have demonstrated antimicrobial properties (Dizaj et al., 2014). Iron oxide (Fe_3O_4) nanoparticles are superparamagnetic and have emerged as promising candidates for biomedical applications such as magnetic resonance imaging probes (Mody et al., 2010).

2.1.3 Polymeric Nanomaterials

In addition to metal and metal oxide nanoparticles, polymeric nanoparticles habe been developed for a variety of applications (Libralato et al., 2017). As one of the most heavily used plastics in daily life, polystyrene is made by the polymerization of styrene monomers. Polystyrene nanoparticles not only inherit the properties of its bulk form, such as biocompatibility and low degradability in the cellular environment, but also have the advantages of unified shape and narrow range of nanoscale size distributions compared to other nanomaterials (Libralato et al., 2017). Polystyrene nanoparticles also have great potential for drug delivery by incorporating ligands for targeting organs. Recently, fluorescent polystyrene nanoparticles have been used in biodistribution tracking and visualizing localization (Markus et al., 2015). Moreover, surface charge can be modified

by coating polystyrene nanoparticles with different functional groups. For instance, the addition of amine groups ($NH2^{-}$) permits the design of cationic polystyrene nanoparticles; while the addition of carboxyl ($COOH^{-}$) groups generates nanoparticles with anionic surfaces. Neutral or negatively charged anionic polystyrene nanoparticles are generally non-toxic to cells; whereas positively charged cationic polystyrene particles able to penetrate cell membranes and are often extremely toxic (Frohlich, 2012).

The stability that polystyrene and other polymeric nanoparticles display makes these particles extremely persistent in the environment. Natural geological and environmental processes mechanically shear polystyrene and other bulk polymers into micro and nanoscale particles which ultimately become incorporated into the cells of living organisms, even the smallest single-cell organisms (Florence et al., 1995). Although the impact of these materials is not completely realized, early research suggests that such micro and nanoscale materials adversely affect a wide range of biological processes (Baun et al., 2008).

2.1.4 Quantum Dots

Quantum dots were first discovered in the 1980's as nanoparticles with semiconducting properties and sizes less than 10 nm in diameter (Jovin, 2003). Similar in some respects to metal oxides, quantum dots are crystalline compositions of semiconductor elements and are fabricated by a top-down or bottom-up approach (Medina and El-Sayed, 2009). Quantum dots also exhibit unique optical and electronic behaviors in a size-dependent manner, which is not found in their bulk forms. The

original quantum dots consist of two parts: a cadmium selenide (CdSe) core and a zinc selenide (ZnS) capping material (Jovin, 2003). However, newer quantum dot materials consist of less toxic materials like carbon (Jelinek, 2017). Quantum dots are fluorescent materials that possess broad excitation spectra, while exhibiting an emission spectrum that is confined into a relatively narrow band (Pisanic et al., 2014). The spectral range of emission is tunable by altering particle size and chemical composition of the core material (Pisanic et al., 2014). Compared with traditional fluorophores such as fluorescein isothiocyanate and rhodamine, quantum dots are more resistant to photobleaching and engineered potential for functionalization. In recent years, a plethora of studies have sought to develop specific binding of quantum dots to target cells/molecules for drug delivery and cellular imaging. Wu et al. have specifically labeled subcellular targets including cell surface receptors, cytoskeletal components, and nuclear antigen with quantum dots conjugated to IgG and streptavidin (Wu et al., 2003). However, the usual core material cadmium is typically highly toxic, which drives recent studies into the direction of seeking biologically safe materials for future technologies. Silicon is considered as the most biocompatible material, and meantime silicon in the form of quantum dots hold great promising properties like nontoxicity and biodegradability (Dohnalova et al., 2014). Thus, quantum dots bring promising novelty to the current field of industry and medicine.

2.2 Nanotoxicity

2.2.1 Summary

In 1990, Oberdörster and Ferin reported that nano-scaled TiO_2 and Al_2O_3 particles induced greater pulmonary toxicity than larger particles through inhalation exposure in rats (Oberdörster et al., 1990). Fourteen years later, the new subcategory of toxicology, “nanotoxicology” was proposed to address the significant influence of nanomaterial after growing attentions in this field (Donaldson et al., 2004).

The main focus of current nanotoxicity is the study of the effects on living organisms of engineered nanoparticles. The greatest challenge of these studies is correlating nanoparticle toxicity with their distinct physical-chemical properties. The large surface area to volume ratio of nanoparticles makes them highly reactive to biological systems (Buzea et al., 2007). Furthermore, nanoparticles exhibit unique properties that differ from their bulk materials, such as quantum effects, electrical, optical, and magnetic behaviors. In addition to these properties, Nanoparticles have uncharacterized interactions with proteins and other biological polymers, moreover many of the mechanisms that control these interactions are completely unresolved. Many nanoparticles rapidly adsorb proteins after entering physiological fluids on their surface and form “protein corona” as multiple biomolecule layers which will alter the properties of the nanomaterial and their interactions with the intracellular/extracellular environment (Bertrand et al., 2017).

Nanoparticles have been shown to induce cytotoxicity, inflammatory response, oxidative stress, genotoxicity, and carcinogenicity *in vivo* and *in vitro.* Here, I briefly

summarize the toxicity evaluation findings of several commonly used metallic and metal-oxide nanoparticles in Table 2 (*in vitro*) and Table 3 (*in vivo*). Next, detailed discussions about the molecular mechanisms underlying nanotoxicity of the most two studied nanoparticles, nanosilver and titanium oxide (TiO_2) nanoparticles, are presented.

Table 2. Results of Commonly Used Metal-based Nanoparticle Toxicity *in vitro* Studies

Nano-particles	Size	Concentration; Incubation time	Cell line	Response	Reference
Gold (Au)	– Length-to-diameter ratio: 4:1	0.4 nM; 96h	HT29	Cytotoxicity	(Alkilany et al., 2009)
	– 15 nm	125 nM, 250 nm; 24 h	HUVEC	Decrease VEFG migration and tube formation	(Pan et al., 2014)
Copper Oxide (CuO)	– Sphere: 40 nm; Rod shape: 10nm/74nm	5 - 100 mg/ml; 24, 48, 120 h	Caco-2 A549 SZ95 N-hTERT	Rod-shaped NPs are more toxic Up-regulation of pro-inflammatory genes	(Piret et al., 2012)
	– 50nm	1-40 µg/ml; 24h	A549 SAEC	Affecting cell cycle Down-regulation of proliferation genes	(Hanagata et al., 2011)
Iron Oxide (Fe_3O_4)	– 10-20nm	100 - 1600 mg/L	*Saccharomyces cerevisiae*, baker's yeast	Inhibit yeast growth by dysfunction of mitochondrial respiratory	(Peng et al., 2018)
	– 15-50nm	2.6 - 26 µg/cm^2	HEK JB6P (+)	Elevated IL-8 and IL-6 cytokines in HEK cells; NF-κB activation under UVB exposure with JB6P (+) cells	(Murray et al., 2013)

Table 2. Results of Commonly Used Metal-based Nanoparticle Toxicity *in vitro* Studies (continues from last page)

Nano-particles	Size	Concentration; Incubation time	Cell line	Response	Reference
Silver (Ag)	– 35nm; <100nm; 2000-3500nm	22, 70, 220, 700, 2200 µg/ml	Human red blood cells	Higher portion of hemolysis for nanosized NPs and concentrations above 220 µg/ml	(Choi et al., 2011)
	– Bio-synthesis: 20nm; Chem-synthesis:35nm	50 µg/ml, 100 µg/ml; 24h	A549	Both NPS exhibit oxidative stress mediated cytotoxicity	(Han et al., 2014)
Titanium dioxide (TiO_2)	– 24nm	1 mg/ml; 1, 2, 3, 24h	HEKn HUVEC	Disrupt intracellular homeostasis ER stress	(Simon et al., 2017)
	– P25:21nm; Rutile: 50nm; Anatase:50nm	25, 50, 100 ppm	Primary rat cortical astrocytes	Mitochondrial dysregulation ROS production A significant loss of glutamate uptake	(Wilson et al., 2015)
Zinc Oxide (ZnO)	– 20nm	10-1000 µg/ml; 4h	Caco-2 SW480	Cell death ROS production Release cytokine IL-8	(Abbott Chalew and Schwab, 2013)

Table 3. Results of Commonly Used Metal-based Nanoparticle Toxicity *in vivo* Studies.

Nano-particles	Size	Dose	Animal mode(Age)	Exposure	Response	Reference
Gold (Au)	– 13.09nm	1000 mg/kg	Female BALB/c mice (5-6 weeks)	Intravenous (Single dose)	Develop granulomas in the liver and increase pro-inflammatory cytokines in serum	(Bahamonde et al., 2018)
	– 5nm	670 nmol/L	Nude mice (6-8 weeks)	Intravenous (two injections every 48h)	Angiogenesis Bind and inhibit the activity of heparin-bind glycoproteins	(Mukherjee et al., 2005)
Copper Oxide (CuO)	– 100nm	400, 700, 1000 ppb	*Mytilus edulis*, Blue mussel	Ingestion	Accumulation mainly in gill Oxidative stress Does dependent toxicity	(Hu et al., 2014)
	– 28nm	5, 10, 15 mg/L	*Caenorhabditis elegans*, Roundworms	Ingestion	Neurodegeneration Reduce reproduction	(Mashock et al., 2016)
Iron Oxide (Fe_2O_3)	– 6.8nm	10 mg/kg	BALB/cJ mice (7-10 weeks)	Intravenous (Single dose)	Accumulation in liver No effect on kidney Decrease blood pressure	(Iversen et al., 2013)

Table 3. Results of Commonly Used Metal-based Nanoparticle Toxicity *in vivo* Studies (continues from last page).

Nano-particles	Size	Dose	Animal mode(Age)	Exposure	Response	Reference
Iron Oxide (Fe_3O_4)	– 35nm	5 – 40 mg/kg	SPF Kunming make mice (8 weeks)	Intraperitoneal injection (Daily for one week)	Hepatic and renal injuries via oxidative stress	(Ma et al., 2012)
Silver (Ag)	– 15nm	179 μg/m³	Rats (10 weeks)	Inhalation (6h/day, 4 days)	Moderate pulmonary toxicity 175-fold increase influx of lung neutrophils	(Braakhuis et al., 2014)
	– 50-60nm	30 mg/kg	*Rattus norvegicus*, Sprague Dawley rats	Intravenous (Single dose)	Induce brain edema formation	(Sharma et al., 2010)
Magnesium Oxide (MgO)	– 20nm	50 – 400 mg/L	*Danio rerio*, Zebrafish	Aquatic	Embryo malformation Cellular apoptosis and intracellular ROS	(Ghobadian et al., 2015)
Titanium dioxide (TiO_2)	– 171nm	10 mg/m3	*Rattus norvegicus*, Sprague Dawley rats	Inhalation (5h)	Increase uterine microvascular sensitivity	(Stapleton et al., 2015)
	–25nm	1, 10,100mg/L	*Danio rerio*, Zebrafish (embryos)	Aquatic (96h)	Accelerate hatching of the larvae	(Clemente et al., 2014)

2.2.2 Overview of Nanosilver Toxicity

Nanosilver is the most commonly used nanomaterial due to its attractive physiochemical properties and most importantly, its antimicrobial property (Schluesener and Schluesener, 2013). The number of consumer products that utilize nanosilver increased dramatically over the last couple of years. More than twenty different types of personal hygiene products such as shampoo, air filters, and water disinfectants alone contain silver nanoparticles, indicating that environmental and human exposure to this nanomaterial is common (Schluesener and Schluesener, 2013). High concentrations of nanosilver have been found in various environmental locations such as the rivers of Texas (Wen et al., 1997) and old silver mining areas of Mexico (Yu et al., 2013). Intentional and unintentional exposure to nanosilver includes ingestion, skin contact, inhalation, and dermal contact. Extreme exposures to nanosilver result in a condition called ‘argyria in which patients develop a bluish or grayish color to their skin after being exposed to nanosilver (Wadhera and Fung, 2005). Given the increasing concerns related to nanosilver, there has been an increase in research of nanosilver-mediated toxicity on a range of different organisms (Chairuangkitti et al., 2013; Dziendzikowska et al., 2012; Massarsky et al., 2014).

2.2.2.1 Factors Influence Nanosilver Toxicity

Although a large amount of research has been performed on the toxicity of nanosilver, the exact mechanisms that underlie the toxic effects of this nanomaterial remain unclear. Researchers have identified several factors that affect the toxicity of

silver nanoparticles, mostly relating to nanoparticles' physicochemical properties. Silver nanoparticles are unstable and serve as a source of silver ions, which have distinct and defined effects on a variety of cellular mechanisms. The instability of the silver nanoparticles delivers higher doses of silver ions to specific cells or tissues, which is hypothesized to be the source of most toxicity induced by silver nanoparticles (Hadrup and Lam, 2014). Given this, several aspects of silver nanoparticles control this stability and therefore silver nanoparticle-mediated toxicity. The size of the particle seems to have a significant impact on toxicity as the smallest size of silver nanoparticles exhibit the highest cytotoxicity in L929 fibroblasts (Park et al., 2011). This result is in agreement with other studies that also demonstrate size-dependent toxicities (Gliga et al., 2014b; Lankveld et al., 2010). Other work has shown that the nanoparticle size is also instrumental for cellular uptake of a nanoparticle (Gliga et al., 2014a) and perhaps the size dependency of silver nanoparticle toxicity is also a function of internalization by a cell. Furthermore, small metallic nanoparticles have been shown to be less stable, which also may contribute to the toxic effects (Jiang et al., 2008). This duality demonstrates a difficulty when interpreting structure/toxicity relationships, as it is often difficult to separate one property (i.e., size) from another property (i.e., stability). The surface charge of silver nanoparticles, which is reflected by zeta potential in the hydrodynamic state, also contributes the antimicrobial effect/toxicity of silver nanoparticles towards gram-negative bacteria (El Badawy et al., 2011). Bacterial plasma membranes are often highly negatively charged (Sondi and Salopek-Sondi, 2004), and particles with highly positive zeta potential may more effectively bind to the surfaces of bacteria, thereby delivering

higher doses of the toxic silver ions. Other properties that have been demonstrated to affect the toxicity of silver nanoparticles include particle shape (Abramenko et al., 2018), the stability and the ability to release silver ion released in the environment (Yang et al., 2012), and exposure time (Dziendzikowska et al., 2012).

2.2.2.2 Biodistribution and Cellular Uptake

Although studies in tissue culture systems allow the determination of acute toxicity and some of the cellular responses to silver nanoparticle exposure, whole animal testing is required to determine both the bio-distribution of nanosilver and subsequent cellular in the tissues that comprise these targets. In many nanoparticle studies, the liver, kidneys, and spleen due to their physiological functions tend to accumulate nanomaterials (Almeida et al., 2011). Silver nanoparticles are processed in a similar manner after both oral and intravenous exposure. After a 28-day oral exposure in mice, nanosilver concentrated mostly in the liver and spleen (van der Zande et al., 2012). Silver nanoparticles intravenously administered after 16-day had similar biodistribution in liver and spleen (Lankveld et al., 2010). These results suggest that reticuloendothelial systems accumulate nano-size particles and that the cells in these organs are most at-risk to high dose exposures of nanosilver. At the cellular level within tissues, the uptake of silver nanoparticles appears to use the same processes as demonstrated by silver nanoparticle uptake in tissue culture cells and primarily involve endocytic processes (Farkas et al., 2011; Scown et al., 2010).

2.2.2.3 Molecular Mechanisms

The cytotoxic effects of nanosilver involve the generation of reactive oxygen species (ROS) (Park et al., 2011). Both *in vitro* and *in vivo* studies have shown that nanosilver induced cytotoxicity was mediated by ROS generation (Chairuangkitti et al., 2013). Gene expression related to oxidative stress was upregulated in the mouse brain after acute exposure to nanosilver intravenous administration (Rahman et al., 2009). Oxidative stress can lead to serious cellular injuries such as DNA damage and apoptotic cell death. Silver nanoparticle exposure produces DNA breakage (Piao et al., 2011), DNA adducts (Foldbjerg et al., 2011), the formation of micronuclei (Kawata et al., 2009) and apoptosis in mammalian cells (Sanpui et al., 2011). Furthermore, silver nanoparticle exposure resulted in the up-regulation of p53 and caspase 3 in human cells (Gopinath et al., 2010). These results demonstrate that the effects of silver nanoparticle exposure active a common and well described ROS mediated signaling pathway, but the manner in which the structure and stability of silver nanomaterial relates to these changes is unclear.

In addition to ROS-mediated stress signaling pathways, several classic signal transduction pathways are also activated by silver nanoparticle exposure. In *C. elegans*, mitogen-activated protein kinase (MAPK) - based oxidative stress signaling pathway is involved after nanosilver exposure (Roh et al., 2012). Also, nanosilver-treated cells displayed decreased EGF-dependent Akt and Erk phosphorylation in human epithelial cells (Comfort et al., 2011). Whether these pathways are part of the stress response (either directly or indirectly) or a parallel/ independent response to nanosilver is unclear.

2.2.3 Toxicity of Titanium Dioxide Nanoparticles

Titanium dioxide (TiO_2) nanoparticles are one of the most produced and commonly used metallic oxide nanomaterials and have been widely applied in the cosmetics, semiconductors, and chemical industries (Shi et al., 2013). TiO_2 nanoparticles are often used as whiteners in paints and papers, and accounts for 70% of the global production volume of TiO_2 nanoparticles (Baan et al., 2006). Smaller TiO_2 nanoparticles possess a high UV absorption capability and have been extensively used in sunscreens (Kiss et al., 2008). The photocatalytic activity of TiO_2 nanoparticles has been used for water purification and water-splitting for hydrogen fuel (Ni et al., 2007). TiO_2 nanoparticles are available in three crystalline phases: anatase, rutile, and brookite (Iavicoli et al., 2012). Anatase TiO_2 nanoparticles have the most chemically reactive crystal structure with a high refractive index and strong absorption of ultraviolet (UV) radiation. In a pulmonary toxicity study in rats (Warheit et al., 2007); anatase TiO_2 nanoparticles also generated higher levels of inflammation, cytotoxicity, and cell proliferation than rutile samples (Grassian et al., 2007; Jin et al., 2008; Park et al., 2008). This result demonstrates that beyond composition, the crystalline organization of a nanomaterial has enormous impacts on its biological effects.

2.2.3.1 Cellular Uptake and Bio-distribution

The cellular uptake of TiO_2 nanoparticles into A549 cells occurs through the clathrin-mediated endocytosis pathway (Tedja et al., 2012). Moreover, exposure to fetal bovine serum not only reduces the aggregation of TiO_2 nanoparticles but also increase the

overall uptake of TiO_2 nanoparticles over 24 h which demonstrates the role of the protein corona. Using TEM, the internalization of both anatase and rutile TiO_2 nanoparticles resulted in the generation of phagosome-like structure in cytosol, however, only the anatase TiO_2 NPs exhibited phototoxicity after UVA radiation (Horie et al., 2016). Again, these results show that internalization of nanomaterials is not completely associated with toxicity and that other properties contribute to toxicity.

Similar to the tissue distribution of nanosilver, the intravenous administration of 20 – 30 nm TiO_2 nanoparticles with a dose of 5 mg/kg resulted in the highest accumulation in the liver and no detectable amount in blood and brain (Fabian et al., 2008). The half-life of TiO_2 nanoparticles in blood is estimated to be 12.7 days, to be eliminated from blood after intravenous injection (Elgrabli et al., 2015). Inhalation exposure accounts for a great proportion of the different routes for TiO_2 nanoparticles to enter into the human body, especially in occupational and incidental circumstances (Leso et al., 2017). Inhalation exposure of rats to TiO_2 nanoparticles showed that a small fraction of the nanoparticles translocated into the connective tissue and also into systemic circulation (Muhlfeld et al., 2007). Through oral exposure with single high dosage (5 g/mg), the TiO_2 nanoparticles were mainly retained in the liver, spleen, kidneys, and lung tissue in rats after two weeks (Wang et al., 2007).

2.2.3.2 Mechanisms of TiO_2 NPs – Mediated Toxicity

Many studies have been done over recent years on the toxicity of TiO_2 nanoparticles, and the findings are valuable in helping us understand the biological

impact and cellular mechanisms underlying the toxicity. TiO_2 nanoparticles triggered an apoptotic response by inducing cellular oxidative stress, activation of cytosolic caspase-3, and chromatin condensation (Park et al., 2008). Furthermore, the ROS generated by the TiO_2 nanoparticle-induced apoptosis did not contain hydrogen peroxide and instead produced high levels of cellular lipid peroxidation and cathepsin B release (Hussain et al., 2010). Furthermore, the ROS production was dependent on the UVA irradiation of TiO_2 nanoparticles (Yin et al., 2012).

The pro-inflammatory response is an important non-specific defense against tissue damage and reported by several studies of TiO_2 nanoparticles exposure. With the combination of ovalbumin injection on mice, TiO_2 nanoparticles increased the level of inflammatory lung cells and stimulated the immune response by the generation of eosinophils (Larsen et al., 2010). Furthermore, Mishra et al. have investigated the adjuvant effect with ovalbumin in a mouse model of asthma and found that TiO_2 nanoparticles exacerbated the inflammatory responses via the NF-κB pathway (Mishra et al., 2016). The inhalation of TiO_2 nanoparticles in newborn rats was also able to stimulate an immune response by upregulating airway neutrophils (Scuri et al., 2010). *In vitro*, Armand et al. have shown the excretion of pro-inflammatory cytokines of 1L-1β and also up-regulation of matrix metalloprotease (MMP) -1 in pulmonary lung fibroblasts (Armand et al., 2013). Some studies have reported genotoxicity and carcinogenesis of TiO_2 nanoparticles exposure. However, the data are conflicting, and the dosage is relatively high. TiO_2 nanoparticles promoted the phosphorylation of histone H2AX and DNA damage (Setyawati et al., 2013). As a further demonstration of large-scale

genotoxic and genomic changes, TiO_2 nanoparticles exposure transformed benign mouse fibrosarcoma cells into aggressive tumor cells (Onuma et al., 2009).

CHAPTER III

CHARACTERIZATION OF NICKEL NANOPARTICLES, IRON-NICKEL ALLOY NANOPARTICLES, AND NICKEL OXIDE NANOPARTICLES

3.1 Introduction

The emergence of nanotechnology has stirred increasing attention in the use of consumer products that contain nanomaterials, especially in the biomedical and semiconductors industries. However, unlike the tradition toxicological assessment of a potentially hazardous material, the risk assessment of nanoparticle toxicity in addition to the identification of the biological impact also requires comprehensive characterizations of the nanoparticles. Nanoparticles exhibit distinct physicochemical properties than the bulk materials to which they are compositionally related and the relationships between the structure and properties of a nanoparticle and its potential deleterious effect are not fully realized. Thus, it is imperative to characterized nanoparticle properties such as particle size, morphology, crystal structure, porosity, chemical composition, surface charge/area/chemistry, solubility, and agglomeration state in order to more fully determine its biological impact (Oberdörster et al., 2005).

The further correlation of those parameters with nanoparticle-mediated biological responses is needed to better elucidate the basis of any given nanoparticle's potential threat to the environment and/or human health. Furthermore, the characterization information from manufactured labels are often different from the evaluations by

researchers (Sayes et al., 2011). The various techniques that are available for nanoparticle characterizations are summarized in Table 4.

Table 4. Characterization Assessment Techniques and Parameters of Nanoparticles.

Parameters	Analytical techniques
Particle size and morphology	Scanning (electron, force, tunneling) microscopy Transmission electron microscopy Dynamic light scattering
Optical response	Raman spectroscopy
Crystal structure	Transmission electron microscopy X-ray diffraction
Surface charge	Zeta potentiometer
Surface hydrophobicity	Water Contact angle measurement
Surface composition	X-ray photoelectron spectroscopy
Surface structure	Atomic force microscopy UV-visible
Surface area	Brunauer-Emmett-Teller
Elemental composition	Inductively coupled plasma mass spectrometry Energy disperse X-ray
Agglomeration state	Dynamic light scattering

Scanning electron microscopy is the simplest and most widely used methodology for characterizing particles (Dhawan and Sharma, 2010). To produce an image, during scanning electron microscopy, a focused beam of electrons probes a specimen's surface with energy ranging typically from 0.2 keV to 40 keV. The interaction of the primary beam with the surface atoms generates several distinct reaction products that are collected point-by-point as the primary electron beam is rastered across the surface. These signals include secondary electrons, backscatter electrons, and characteristic X-rays and each signal requires a different detector within the microscope. Images are generated after a detector receives all the interaction signals from a scanned region of interest and after a distribution map of the signal intensity is composed via software into a final digital image (Stokes and Royal Microscopical, 2008). Scanning electron microscopy is a relatively fast imaging process that provides a detailed three-dimensional and topographical image of a sample with resolution below 2.5 nm. However, scanning electron microscopy requires dehydrated samples and therefore does not permit the examination of many biological materials which are often aqueous in nature. Furthermore, the interrogation of a sample with a high energy electron beam and in high vacuum may also generate artifacts and alter the properties of unstable or sensitive nanomaterials. Thus, scanning electron microscopy must be used with other characterization techniques for the comprehensive evaluation of a nanomaterial.

Dynamic light scattering (DLS) is used for evaluating the size distribution profile of small particles in suspension or solution (Goldburg, 1999). The monochromatic light from the Dynamic light scattering laser strikes the small particles that are suspended in an

aqueous medium; the scattering of this light fluctuates over time and, since the fluctuation is due to the Brownian motions of small molecules in solution, the Stocks-Einstein relation can be applied to calculate particle size based on dynamic information. DLS measures the hydrodynamic diameter of a nanoparticle in solution and calculates both intensity and particle number (Kokhanovsky, 2009).

Another important property of nanoparticles in solution is the zeta potential. The zeta potential is also known as electrokinetic potential and is the net charge value between a material's solid surface and liquidous medium. A double layer of ions (known as the Stern layer) exists at the charged interface of a particle in solution, with an inner region of tight binding of the surface of the particle (this is essentially an immobile layer of ions) and an outer region of random ion distribution. A zeta potential is determined by dynamic electrophoretic mobility and reflects the stability and effective surface charge of a nanoparticle in suspension medium (Bhattacharjee, 2016).

Among different types of metal-based nanoparticles, nickel related nanomaterials have unique electrochemical and magnetic properties which enable them to be used as electrode materials, efficient catalysts, conductive pastes, magnetic recording materials, and combustion additives (Pang et al., 2009). As new trending nanomaterials, nickel-based nanomaterials have been investigated frequently over past several years. Tee and his colleagues incorporated nickel nanoparticles into human mimic skin and created novel properties of self-healing and conducting, which firstly allowed artificial skin to sense pressure (Tee et al., 2012). However, several cases of nickel toxicity from

occupational exposure have been reported and require our attention for further investigation (McConnell et al., 1973; Phillips et al., 2010).

The aim of my study was to characterize the size and morphology of the nanomaterial that I used in my research, specifically Nickle/Ni nanoparticles, Nickle/Iron alloy/NiFe nanoparticles, and Nickle oxide/NiO nanoparticles using SEM. I measured the size distribution and aggregation state in aqueous suspensions using dynamic light scattering and finally, determined zeta potentials of the hydrodynamic forms of these nanoparticles.

3.2 Materials and Methods

3.2.1 Materials and NPs Dispersion

Commercial Nickle/Ni nanoparticles, Nickle/Iron alloy/NiFe nanoparticles, and Nickle oxide/NiO nanoparticles were purchased from Sigma Aldrich (Sigma, St Louis, MO, USA). <100> silicon wafers for the mounting of these materials for scanning electron microscopic analysis were purchased from Ted Pella (Ted Pella Inc, Redding, CA. Nanoparticles suspensions were prepared using sterile deionized (DI) water in the stock concentration of 10 mg/ml. The particle suspensions were then diluted into desired concentrations and dispersed for 30 minutes.

3.2.2 Sample Preparation and Imaging with Scanning Electron Microscopy (SEM)

Droplets of 10 µg/ml nanoparticle suspensions were added onto silicon wafers and samples were immediately exposed to an acetonitrile dehydration incubation

chamber for 5 minutes. After drying, the samples were coated with 5 nm gold-palladium using a Leica EM ACE200 glow coater/sputter coater with real-time thickness monitoring by a quartz crystal microbalance technique. To visualize the shape and size of Nickle/Ni nanoparticles, Nickle/Iron alloy/NiFe nanoparticles, and Nickle oxide/NiO nanoparticles I performed scanning electron microscopy using a Zeiss Auriga FIB/SEM. Secondary electron images were collected using a primary electron beam of 3.00 kV with 5.00 mm of WD and detected with the InLens detector. To quantify the sizes of the nanoparticles, I analyzed the scanning electron micrographs using Image J software (NIH). Particle sizes were measured across the largest diameter.

3.2.3 Dynamic Light Scattering

Nickle/Ni nanoparticles, Nickle/Iron alloy/NiFe nanoparticles, and Nickle oxide/NiO nanoparticle suspensions were prepared in the concentrations of 10, 50, 100, 500, and 1000 µg/ml from a stock solution using DI water. No additives or dispersing solvents were added to these solutions. Therefore, all of these measurements were of native nanoparticle interactions in water. After a 30-minute sonication, I measured device hydrolytic particle size and zeta potential of Nickle/Ni nanoparticles, Nickle/Iron alloy/NiFe nanoparticles, and Nickle oxide/NiO nanoparticles using a DLS instrument (Zetasizer Nano-ZS, Malvern Instruments, United Kingdom). All measurements were conducted at 25 °C.

3.3 Results and Discussion

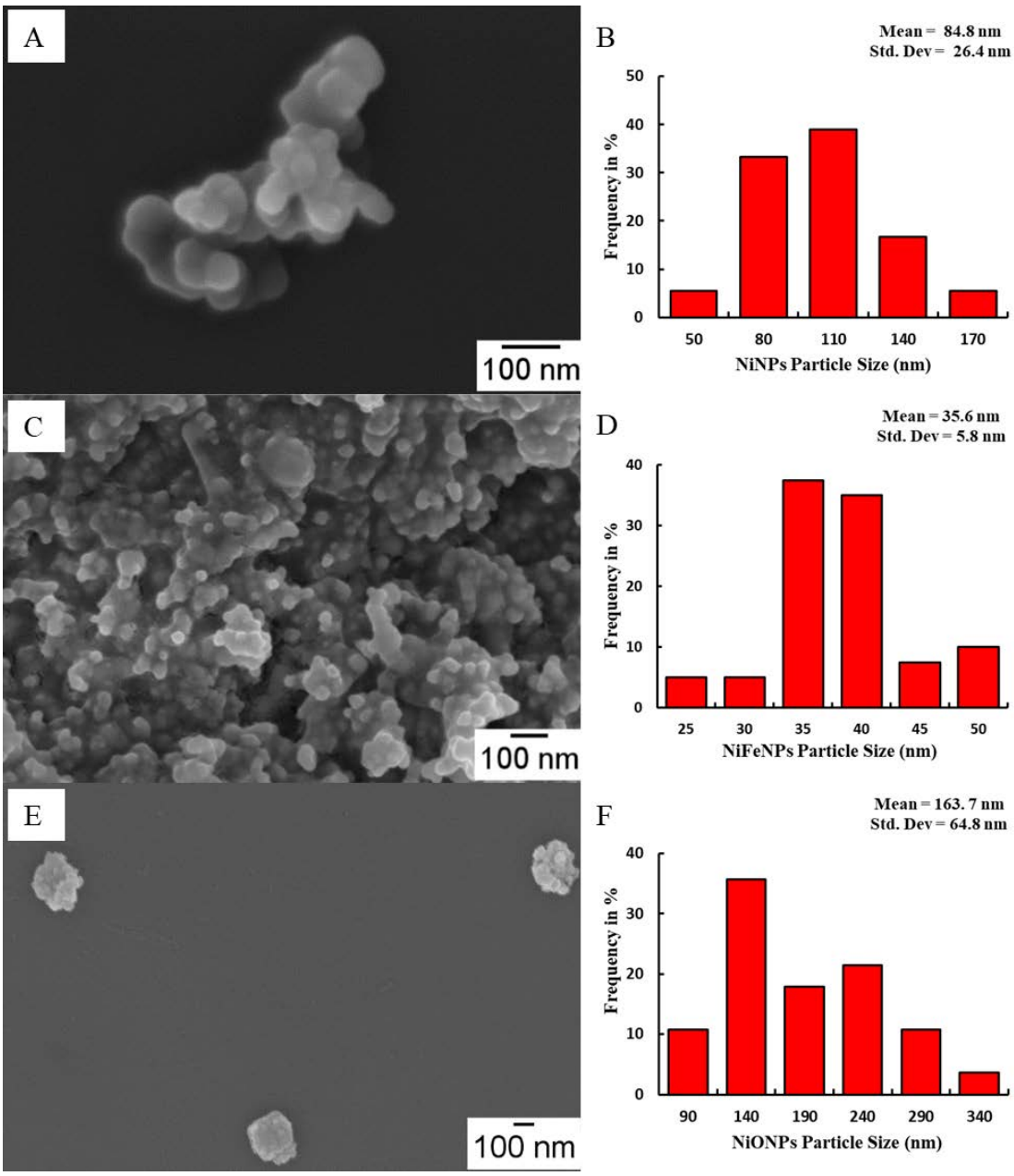

Figure 5. Characterization of Nanoparticles using Scanning Electron Microscopy. Size and morphology of Nickel/Ni nanoparticles (A), Nickel/Iron alloy/NiFe nanoparticles (C), and Nickel oxide/NiO nanoparticles (E) are presented in electron microscopy images. Measured diameters are quantified for size distribution with sample size of n = 30 (B, D, E). Abbreviation: NPs, nanoparticles.

Table 5. Physicochemical Characteristics of Studied Nanoparticles. BET: Brunauer–Emmett–Teller; TEM: Transmission electron microscopy; NPs: nanoparticles

Nominal Diameter (nm)		Ni NPs	NiFe NPs	NiO NPs
Manufactured Size		<100 nm	<100 nm (BET)	<50 nm (TEM)
SEM Diameter (nm ± SD)		84.8 nm ± 26.4 nm	35.6 nm ± 5.8 nm	163.7 nm ± 64.8 nm
DLS size of primary peak (nm)	10 μg/ml	13.54 nm	1365 nm	349 nm
	100 μg/ml	405.1 nm	1621 nm	363 nm
	1000 μg/ml	900.7 nm	1186 nm	885 nm
Zeta Potential (mV)		− 9.86 mV	− 8.42 mV	21.5 mV

The physical properties of three different nanoparticles were tested prior to addition into the fly culture medium. Nickle/Ni nanoparticles and Nickle/Iron alloy/NiFe nanoparticles displayed spherical shapes (Figure 5 A, B), whereas Nickle oxide/NiO nanoparticles exhibited polyhedral shapes (Figure 5 E). Quantifications of the size distribution based on SEM images show that diameters of Nickle/Ni nanoparticles, Nickle/Iron alloy/NiFe nanoparticles, and Nickle oxide/NiO nanoparticles are 84.8, 35.6, and 164.7nm, respectively. Compared to the suggested sizes from manufacture labeling (Table 5), Nickle/Ni nanoparticles and Nickle/Iron alloy/NiFe nanoparticles are consistent with manufacturing forms. However, Nickle oxide/NiO nanoparticles are approximately three times larger than manufactured size. In another study by Morimoto et al., agglomerates of Nickel oxide/NiO nanoparticles under SEM were also detected with the size of 480 nm (Morimoto et al., 2012), which is in agreement with our findings. Another metal-oxide nanoparticle, Magnesium oxide/MgO nanoparticles, also had similar aggregates under SEM (Ghobadian et al., 2015). Nickel oxide/NiO nanoparticles exhibit better solubility than Nickel/Ni nanoparticles and Nickel/ Iron alloy/NiFe nanoparticles when suspended in DI water and it is also possible that they clump more by the water evaporation during the sample preparation process.

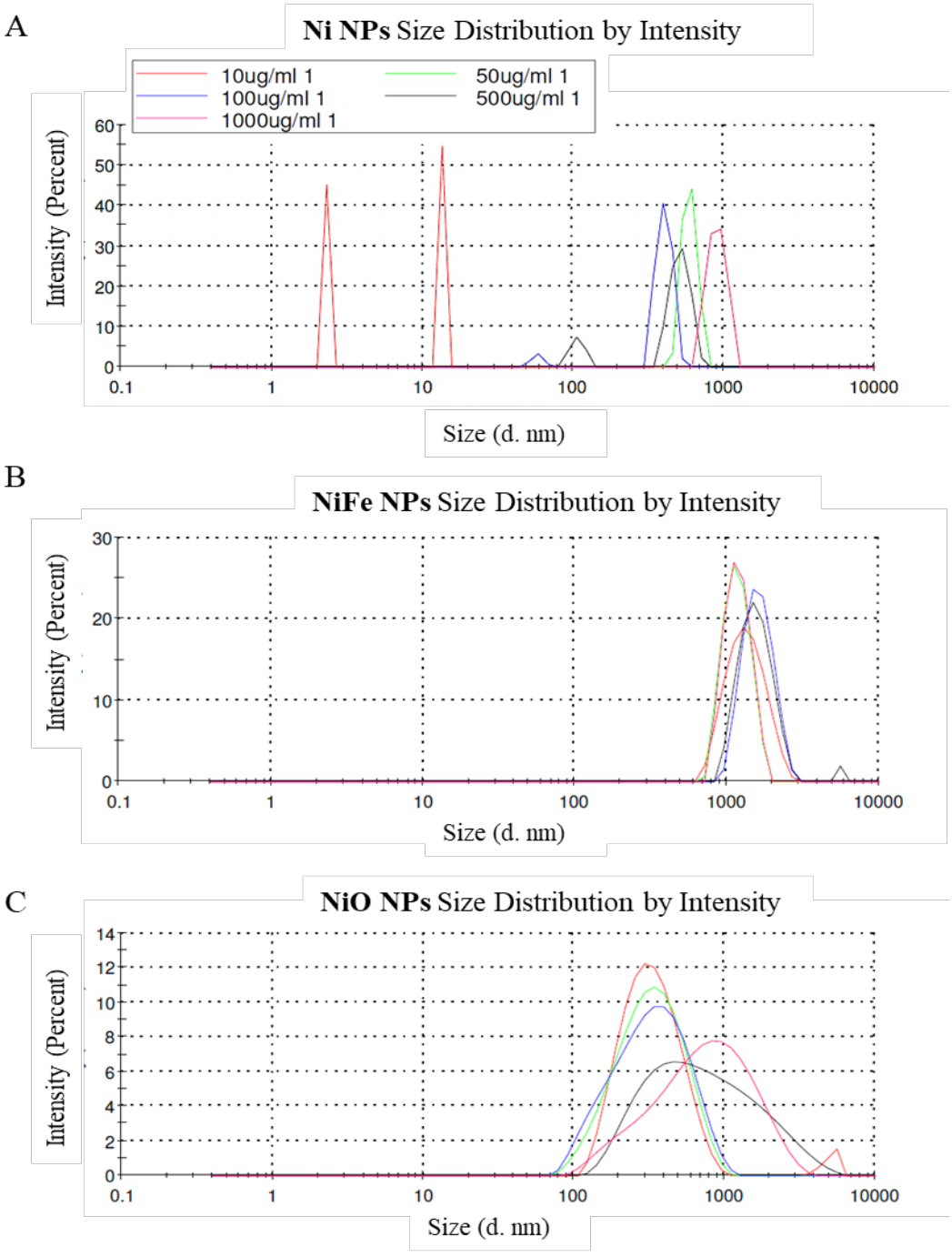

Figure 6. Hydrodynamic Size Distribution at Different Concentrations of Suspended Nickel-based Nanoparticles. 10, 50, 100, 500, 1000 µg/ml of Nickel/ Ni nanoparticles (A), Nickel/Iron alloy/NiFe nanoparticles (B), and Nickel oxide/NiO nanoparticles (C) suspensions were prepared in deionized water and sonicated. Abbreviation: NPs, nanoparticles.

Using DSL, I measured the hydrodynamic sizes of the three test nanoparticles in the aqueous state in DI water with increasing concentrations of 10, 50, 100, 500, and 1000 µg/ml (Figure 6). Nickle/Ni nanoparticles show a monodispersed form at the lowest concentration of 10 µg/ml with an average size of 13.54 nm (Figure 6A). This result is similar to published TEM experiments, which measured a wide range of 10 nm – 100 nm for nickel nanoparticles (Song et al., 2008). It has been suggested that the synthetic method contributes to the size and nature of the nanoparticles in solutions; a particular type of synthesis using electric explosion seems to contribute to a broad size range and distribution of nickel nanoparticles (Kotov, 2003). When the concentrations of Nickel/Ni nanoparticles were below 500 µg/ml, one or two intensity peaks were detected: a small fraction of nanoscales particle in a monodispersed suspension and a large fraction of micronized agglomerates (Figure 6A). As the concentration of Nickel/Ni nanoparticle increases to 1000 µg/ml, a single peak with a diameter of 900.7 nm was observed (Figure 6A). The hydrodynamic diameters of Nickel/Iron alloy/NiFe nanoparticles in suspension increases in a dose-dependent manner (Figure 6B). Lastly, Nickel oxide/NiO nanoparticles exhibit relatively similar hydrodynamic sizes across all concentrations (Figure 6C). This may explain the observation that Nickel oxide/NiO nanoparticles exhibit irregular shapes and appeared to agglomerate under SEM analysis. Overall, size measurement as determined by DLS were generally larger than the sizes determined by SEM. This can be attributed to the fact that the Brownian motion fluctuation indicates the mean hydrodynamic radius, which is usually larger than other measurement methods such as SEM, TEM, and BET (Hradil et al., 2007). In addition, during the measurement

process, nanoparticles have a tendency to aggregate in solution over time. Thus, DLS demonstrated the size of clustered nanoparticles in solution rather than monodispersed nanoparticles and this measurement most likely represents the state of these particles in all aqueous solutions including food.

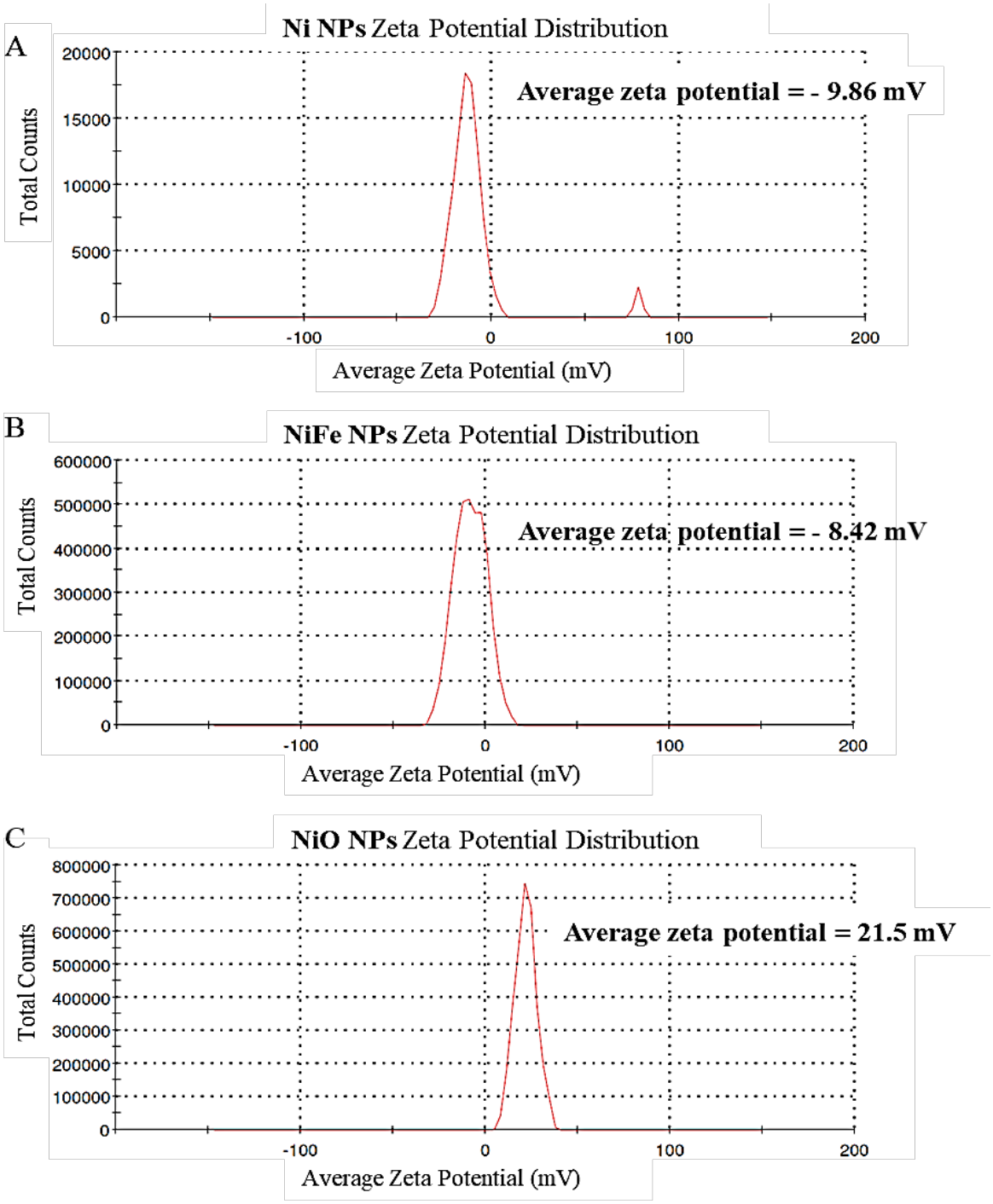

Figure 7. Zeta Potential Measurements of Nickel-based Nanoparticles. The hydrodynamic surface charge of Nickel/Ni NPs (A), Nickel/Iron alloy/NiFe NPs (B), and Nickel oxide/NiO NPs (C) were measured in the concentration of 100 µg/ml. Abbreviation: NPs, nanoparticles

Zeta potential distributions are presented in Figure 7 with suspended concentrations of 100 µg/ml. Both metallic nickel and nickel-iron alloy nanoparticles have average zeta potentials falling in the most active range of ± 10mV, indicating that attractive forces between nanoparticles in the suspension is possible to exceed their repulsion and undergo rapid coagulation or flocculation (O'Brien et al., 1990); whereas nickel oxide nanoparticles belong to the secondary active level of incipient instability between ±10 mV and ± 30 mV. Thus, the different zeta potential levels of metallic nanoparticles and metal-oxide nanoparticles (Figure 7) can also explain the various changes of DLS measurements in nickel and nickel-iron alloy and relatively stable size distributions in nickel oxide nanoparticles with different concentrations (Figure 6).

3.4 Conclusions

In summary, based on the characterization results from this study, I show that that the metallic nickel, nickel-iron alloy, and nickel oxide nanoparticles have distinct properties. Each has a unique size, morphology, and behavior in aqueous solutions. The sample preparation for SEM imaging alters physical properties compared to the manufactured form. The hydrodynamic sizes of nanoparticles did not necessarily increase with concentrations and this behavior suggests that these particles have different chemical activities. Zeta potential data indicates that the nickel oxide nanoparticles I used for my experiments are more electronic stable than either the metallic nickel or the nickel-iron alloy nanoparticles.

CHAPTER IV

COMPARISON OF TOXICOLOGICAL EFFECTS OF NICKEL RELATED NANOPARTICLES USING *DROSOPHILA MELANOGASTER*

4.1 Introduction

Nanoparticles are objects with at least one dimension smaller than 100 nm and can be formed through a variety of natural and synthetic processes (National Nanotechnology Initiative, 2006). The increase in the application of nanomaterials in the fields of biomedicine, industry and agriculture has led to a subsequent increase in the potential exposure of the environment to engineered nanoparticles. This has raised numerous concerns about the risk of side effects on human health. Among various engineered nanoparticles, metallic and metal oxide nanoparticles have been widely used in many fields including solar cells, electronic devices, catalysts, drug delivery and also food additives (Pareek et al., 2017). While contributing to global economy, the manufacturing process of metallic and metal oxide nanoparticles requires high energy and resources and creates numerous wastes. Therefore, there is a compelling need to assess the toxicity of nanomaterials. Nickel and nickel compound nanoparticles have been gaining increasing attention due to their novel characteristics such as high surface energy, high magnetism, low melting point, and low burning point (Ahamed, 2011). For example, researchers are optimizing nickel nanoparticles for drug delivery system in therapeutics (Prijic and Sersa, 2011). Green and novel synthesis of nickel nanoparticles are constantly

being improved (Wu et al., 2010). However, nickel-based nanoparticles have been shown to exhibit biological effect both *in vitro* and *in vivo*. After functionalization with a positive charge on the surface, nickel nanoparticles show increased uptake by hepatocellular carcinoma cells (Guo et al., 2009). Intravenous injection of nickel nanoparticles induces genotoxicity in rats (Magaye et al., 2012).

As an *in vivo* model organism, fruit fly *D. melanogaster* has been used in toxicological studies of several types of nanoparticles (Pappus and Mishra, 2018). TiO_2 nanoparticles were reported to induce dose-dependent genotoxicity using the comet assay in *D. melanogaster* hemocytes (Carmona et al., 2015a). Genotoxicity of copper oxide nanoparticles was also reported in *D. melanogaster*, which was analyzed using a wing spot assay to detect frequencies of mutant spots on adult wings after nanoparticle ingestion (Carmona et al., 2015b). Silver nanoparticles delayed *D. melanogaster*'s development and reduced its reproduction (Philbrook et al., 2011). *D. melanogaster* not only offers physiology and genetic conveniences for investigating nanoparticle toxicity, but also provides advantages such as a short life cycle, easy for manipulations, and high similarities of its GI tract with mammalian intestines. However, more toxic evaluations of nanoparticles are still needed.

Here, we address the question that what is the impact and mechanisms of nickel-based nanoparticles on viability and development of *Drosophila melanogaster* larvae after oral exposure.

4.2 Materials and Methods

4.2.1 Materials

Commercial metallic nickel nanoparticles (<100 nm), Ni particles (< 50 μm), nickel-iron alloy nanoparticles (<100 nm), and nickel oxide nanoparticles (<50 nm) were purchased from Sigma Aldrich (Sigma, St Louis, MO, USA). Dihydroethidium (DHE) dye to measure ROS, and chemical Permount mounting medium were provided by ThermoFisher Scientific.

4.2.2 *Drosophila* Husbandry, Breeding, and Larval Selection

The Canton-S wild-type strain of *Drosophila melanogaster* was obtained from Bloomington stock center and was used for all experiments. *Drosophila melanogaster* adult will be reared on standard cornmeal-meal-yeast medium at 25℃. To measure the effects of nickel nanomaterials on viability and fecundity, I took one-week old male and female flies that had been reared on a yeast-based medium in 100 ml plastic beakers and collected eggs on 60 mm grape juice agar plates every 4-hours (Featherstone et al., 2009). Second instar larvae were collected after 2-3 days for experiments. 10x stock solution (1, 5, 10mg/ml) of Nickle/Ni nanoparticle, Nickle/Iron alloy/NiFe nanoparticles, and Nickle oxide/NiO nanoparticle solutions were freshly prepared and sonicated for 30 minutes to reduce aggregation. The final concentration of each type of nanoparticles was prepared by diluting the stock solution in fly media to the concentrations of 100, 500, and 1000 μg/ml. Third instar *Drosophila melanogaster* larvae were fed with nanoparticle diets: thirty larvae per vial and at least three replicates were set up for each concentration.

Drosophila melanogaster larvae in control group were fed with the same diet without nanoparticles.

4.2.3 Survivorship Assay

After 3 weeks of exposure to the nanoparticle diet, adult *Drosophila melanogaster* were anesthetized with carbon dioxide gas and the number of eclosed adults were counted. The percent survivorship was determined as the number of alive adults divided by the total number of second instar larvae with which I began the experiment.

4.2.4 Larval Development Duration Measurement

Larval development (specifically entry into pupariation) was monitored by counting the number of pupal cases on the glass of each vial every 24 hours. The quantification of developmental delay was also determined by eclosion period. The number of eclosed adults were counted daily.

4.2.5 Wing Size Measurement

The wing size of *Drosophila melanogaster* adults treated with nanoparticle diets was used as a criterion to evaluate their growth and development. The right wings of adult flies were removed and mounted on a slide using Permount. Images of each wing were captured at 50x magnification using ZEISS Axio Imager Microscopy, and the average wing surface area was determined using Image J (NIH).

4.2.6 Confocal Microscopy and Fluorescent Staining

4-day old *Drosophila melanogaster* larvae were inverted and dissected in 1X PBS (137 mM NaCl, 2.7 mM KCl, 4.3 mM Na_2HPO_4, and 1.47 mM KH_2PO_4). To examine the effects of nickel nanomaterials on the larval gut morphology of *Drosophila melanogaster*, larval guts were fixed with a 4% paraformaldehyde solution in 1X PBS and then stained with a combination of 4',6-diamidino-2-phenylindole (DAPI, Excitation/Emission: 358/461 nm) to examine the placement and size of the nuclei, and Alex488 Phalloidin (Excitation/Emission: 495/518 nm) to examine the actin cytoskeleton. Larval tissue was then washed three times with 1X PBS and mounted on slides. Images were taken using Zeiss Z1 Spinning Disc confocal microscope.

To examine the viability of the gut cells and the gut microbiome in larval *Drosophila melanogaster* midguts, the tissue was stained with acridine orange (AO, Excitation/Emission: 500/526 nm) and propidium iodide (PI, Excitation/Emission: 535/617 nm). Staining procedures were similar as described above except larval guts were not fixed. Images were captured immediately after the washing and mounting steps.

After 4-5 days of exposure to nickel nanoparticle containing medium, *Drosophila melanogaster* larvae were inverted, dissected in 1X PBS, and placed into 1 ml of Schneider *Drosophila* media with 10 % FBS for optimal respiration. 0.5 µl of reconstituted Dihydroethidium (DHE, Excitation/Emission: 518/605 nm) dye and 1 µl DAPI were added and gently swirled for 5 min in the dark at room temperature. Larval tissue was then washed three times with Schneider media for 5 min each. The inverted

larval tissue was mounted on a glass slide and images were captured using a Zeiss Z1 Spinning Disk Confocal Microscopy.

4.2.7 Western Blots of *Drosophila Melanogaster* Larvae

Larvae were collected after 4 days of exposure to nickel nanomaterial containing food and control food. Control groups were divided into two groups: a positive control, which was incubated at 37℃ for 2 hours to activate endogenous Hsp70, and a negative control, which was not induced with any stress. All larvae (positive control, negative control and experimental larvae fed nickel nanomaterial diets) were washed to remove extra food, homogenized thoroughly in 10 µl of 1X PBS, and then mixed with a 2X loading protein buffer. Standard SDS-Page analysis was performed as described by Schagger (Schägger, 2006). The following antibodies were used for this analysis: anti-Hsp70 (2A4, 1: 10,000; ThermoFisher Scientific) and anti-β-tubulin (E7, 1:1000; Developmental Studies Hybridoma Bank) antibodies; Secondary antibodies were goat anti-mouse and goat anti-rabbit coupled to horseradish peroxidase (HRP, 1: 4,000, Boehringer).

4.2.8 Statistical Analysis

All experiments included at least three biological replicates, with each containing 30 third instar larvae for each replicate. Statistical Analysis was performed using Microsoft Excel software (Microsoft Corporation, Redmond, DC, USA). One-sided Student’s t-test was used to determine the significance of the difference between the

experimental groups and control groups and a value of $p < 0.05$ was considered as statistically significant.

4.3 Results and Discussions

4.3.1 Survivorship

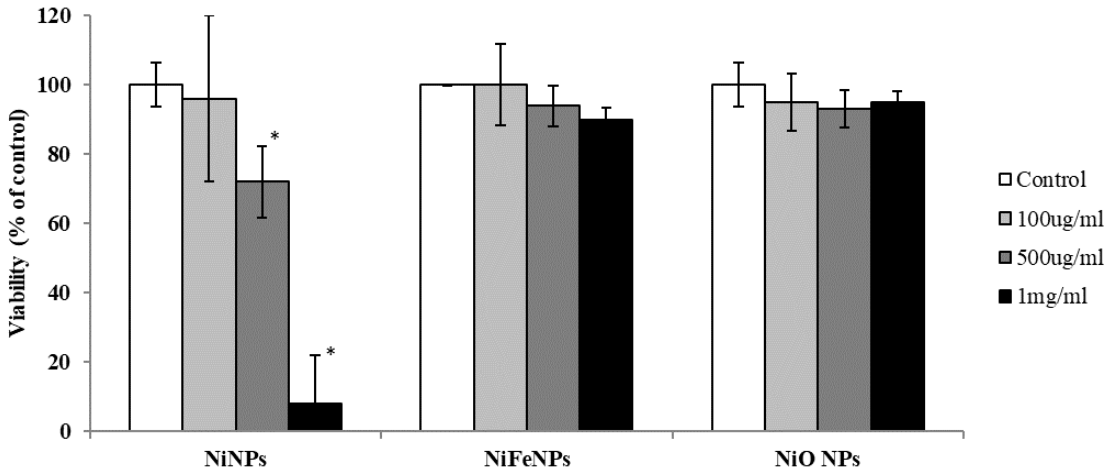

.

Figure 8. Ingestion of Nanoparticles Decreases Viability of *Drosophila melanogaster*. *Drosophila larvae* were reared on standard medium containing different concentrations of nanoparticles. Standard deviations are indicated as error bars. Student t-test was performed to analyze statistical significance. *$p < 0.05$.

I tested the viability of Drosophila larvae exposed to different concentrations of Nickle/Ni nanoparticles, Nickle/Iron alloy/NiFe nanoparticles, and Nickle oxide/NiO nanoparticle. Metallic nickel nanoparticle had a deleterious effect on *Drosophila melanogaster* viability. Larvae fed a corn/agar medium containing 500 or 1000 µg/ml of metallic nickel nanoparticles exhibited reduced viability with 28% and 92% lethality respectively (Figure 8). Fly larvae fed either Nickle/Iron alloy/NiFe nanoparticles or Nickle oxide/NiO nanoparticle didn't show any decrease of viability (Figure 8). Our *in vivo* results are consistent with previous studies, as Nickle/Iron alloy/NiFe nanoparticles showed little toxicity in endothelial cells (Hahn et al., 2012). However, we are the first group to demonstrate that nickel oxide nanoparticles can be nontoxic using our assay system, i.e. oral exposure in *D. melanogaster*. Previous work has suggested that both the *in vivo* intratracheal instillation in rats and *in vitro* exposure in epithelial cells of nickel oxide nanoparticles results in a pathological effect and cell death (Dumala et al., 2018; Latvala et al., 2016). However, in these experiments the administration concentrations are 500mg/kg *in vivo* and 1mg/ml *in vitro*, which are relatively high. Solubility of nickel oxide nanoparticles is a pivotal factor in causing *in vitro* cytotoxicity, which may explain the lack of cytotoxicity in my studies. It is likely that the nanoparticles are more soluble in the *in vitro* cell based assays, than in the *Drosophila* oral delivery system. On the other hand, in another study nickel oxide nanoparticles were able to quench DPPH free radicals in a time-dependent manner, functioning as antioxidant (Saikia et al., 2010). This finding suggests that nickel oxide nanomaterials may operate either in a positive or negative fashion (i.e. as an antioxidant) and in a context-dependent manner. To determine the

impact of the size of nickel nanomaterials on survivorship, *D. melanogaster* larvae were fed a bulk form of nickel material with particle sizes of 50 µm. Although the same concentration of bulk form and nanoscale nickel particles were administered to *D. melanogaster* larvae through oral ingestion, the bulk form did not result in any of the decrease in viability that nickel nanoparticles exhibited (Figure 9).

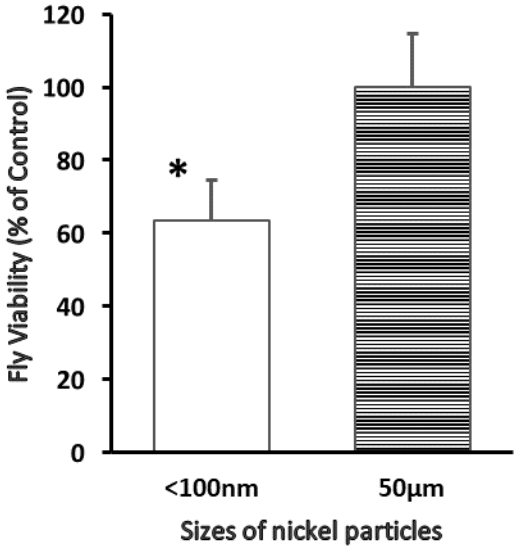

Figure 9. Viability Comparison of Two Different Sizes of Nickel Particles After Oral Exposure with a Concentration of 500 µg/ml in Wild-type *D. melanogaster*. Standard deviations are indicated as error bars. Student t-test was performed to analyze statistical significance. *$p < 0.05$.

4.3.2 Development Delay and Body Size Decrease

I noticed that larvae that survived the exposure to nickel nanoparticle treatments frequently had difficulties to pupariation or enclosure to adults when compared to control larvae, Nickle/Iron alloy/NiFe nanoparticles, and Nickle oxide/NiO nanoparticle treatments. This suggested a delay in development. To characterize this phenomenon, I measured the duration of pupariation for larvae fed with different concentrations of nickel nanomaterials (Figure 10). I observed that larvae in the group fed metallic nickel nanoparticles exhibited a significantly extended time to pupation in a dose-dependent manner (Figure 10). Neither Nickle/Iron alloy/NiFe nanoparticles or Nickle oxide/NiO nanoparticle treated flies showed this effect.

I also measured the surface area of wings from the rare adult flies that survived feeding the nickel nanoparticle diet; the intention was that this measure serves as a general representation of adult body size. Paralleling the results from the pupariation measurements, wing area of emergent adult flies from the nickel nanoparticle diet group differed significantly from those of control groups, the Nickle/Iron alloy/NiFe nanoparticle diet group, and the Nickle oxide/NiO nanoparticle group (Figure 11).

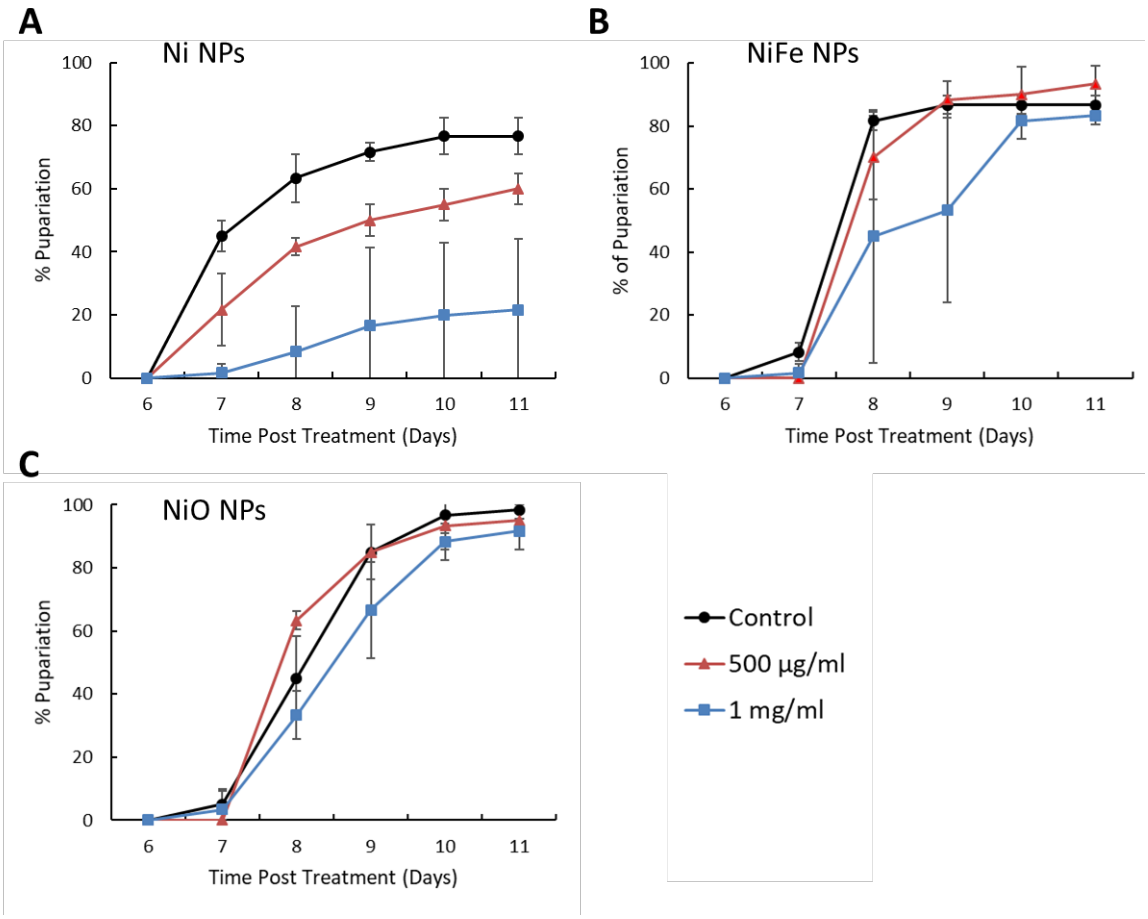

Figure 10. Developmental Time Course of *Drosophila* after Nanoparticles' Ingestion. The percentage of larvae that pupariated were plotted relative to the time in days after nanoparticles' diet. (A) Addition of nickel nanoparticles into the fly medium is sufficient to delay the timing of pupariation. (B and C) No significant effect on Drosophila larvae when exposed to iron-nickel alloy nanoparticles and nickel oxide nanoparticles. Error bars represent S.D. of three independent replicates.

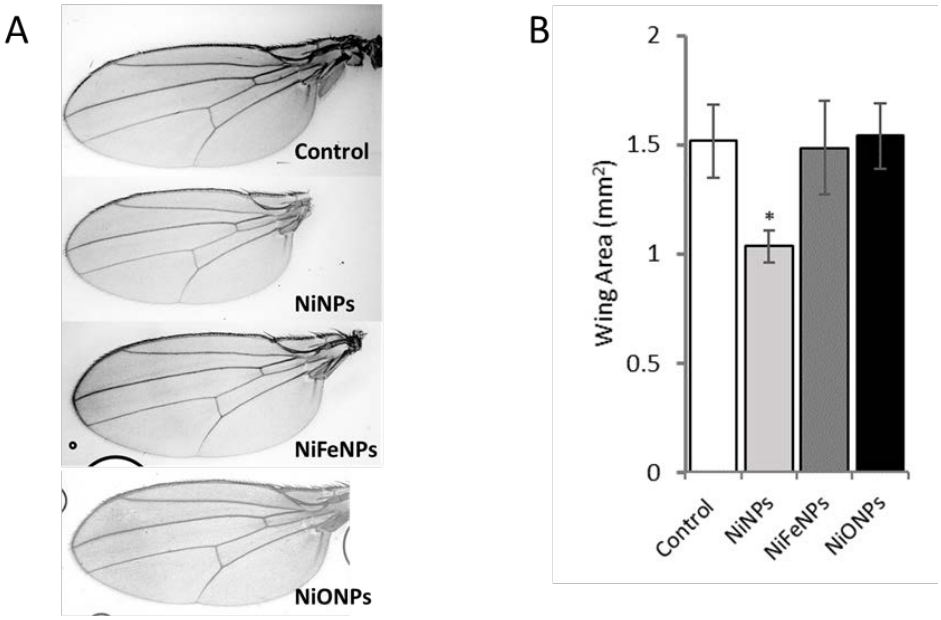

Figure 11. The Dramatic Decrease of Wing Size after Nickel Nanoparticle Dietary Uptake in *D. melanogaster.* A) Brightfield microscopy images of adult wings. B) The surface area of adult wings was quantified. Exposure concentration is 1mg/ml. Standard deviations are indicated as error bars. Student t-test was performed to analyze statistical significance. *$p < 0.05$. Examples of individual fly wings are presented on the right.

Previously studies reported that oral ingestion of TiO_2 nanoparticles negatively affected the growth and viability of *Drosophila melanogaster* imaginal disc cells resulting in smaller wing size and cell death (Carmona et al., 2015a). In another study, accumulation of gold nanoparticles in the fat body of fly larva associated with increased lipid levels and synthesis of *Drosophila* (Wang et al., 2012). Thus, it is possible that during the process of metamorphosis, embryonic and larval tissues, such as imaginal discs, were damaged by nickel nanoparticle treatment in our studies.

4.3.3 Decreasing Abundance of Gut Microbial

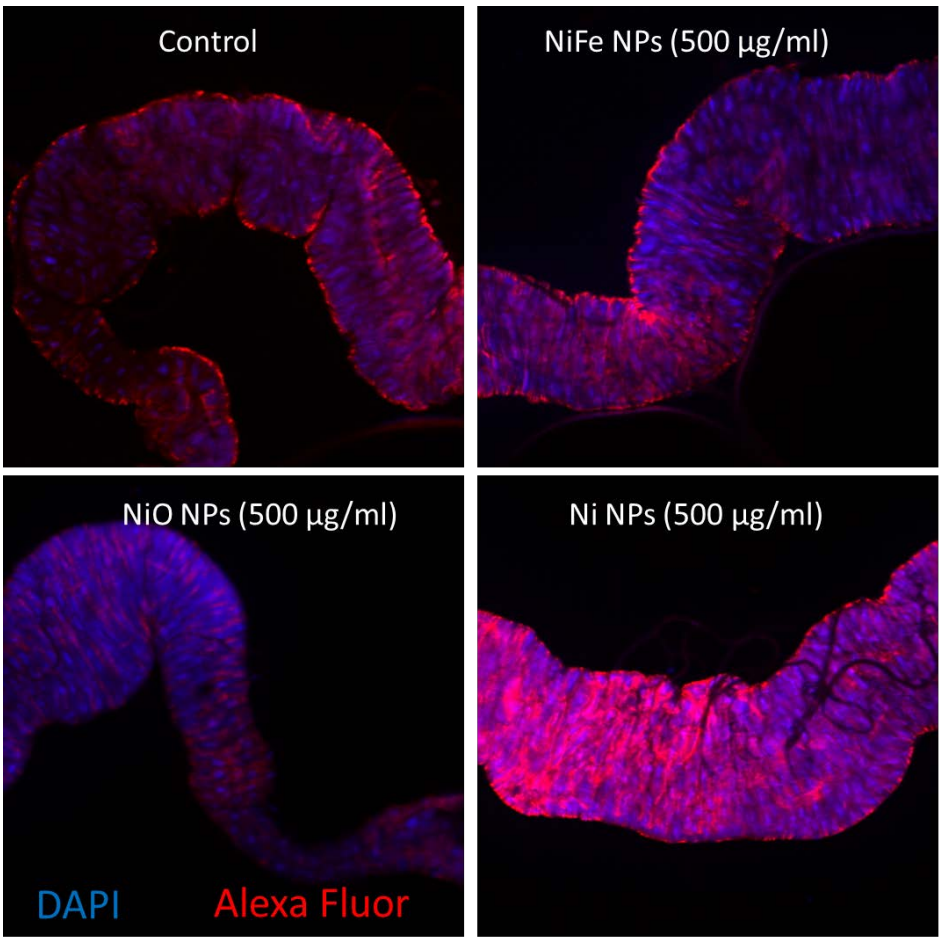

Figure 12. Third Instar Larval Midgut Morphology Remains Unchanged after Ingestion of Nickel-based Nanoparticle under a Confocal Microscope. Gut tissue was stained with DAPI and Alexa 488 phalloidin for visualization of gut morphology.

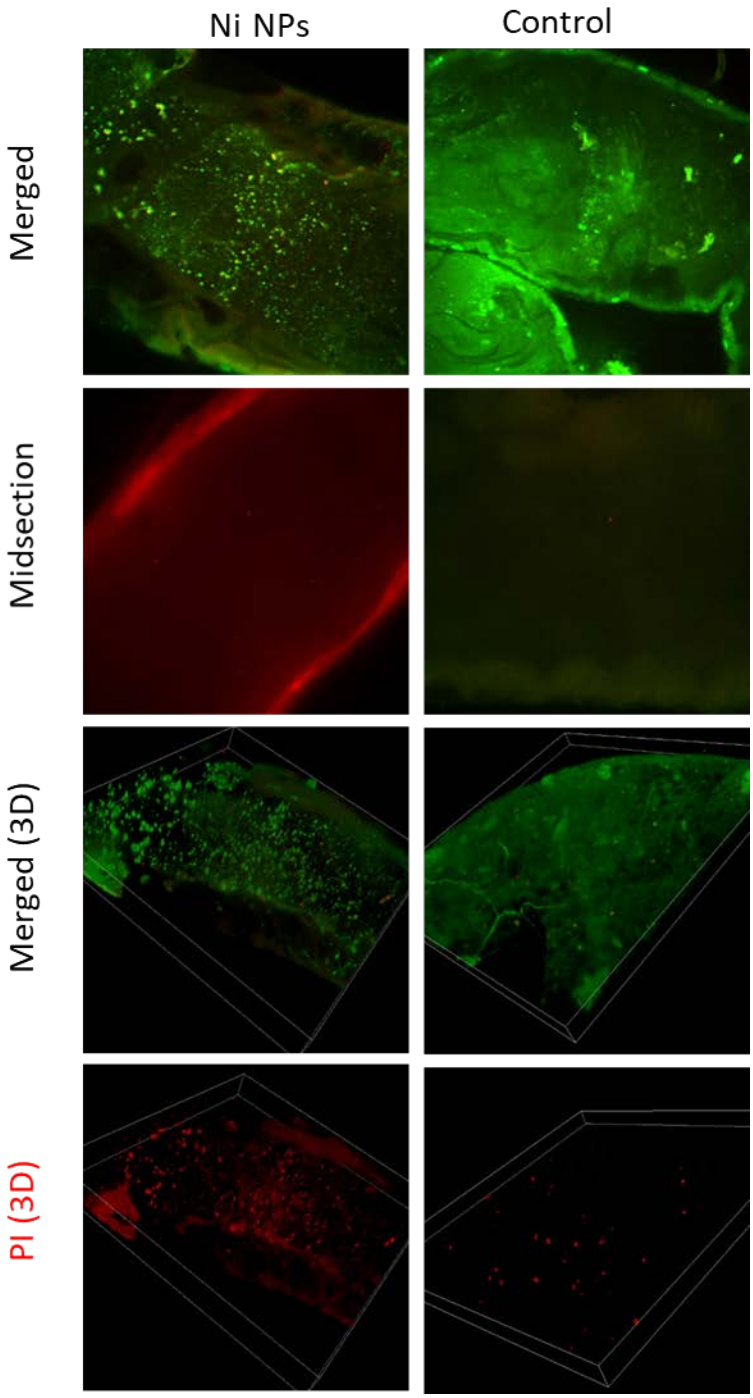

Figure 13. Death Ratio Increased after Nickel Nanoparticle Ingestion in 3rd Larvae Midgut. AO/PI staining of larval midgut under confocal microscope. Red staining indicates dead cells whereas green staining indicates both live and dead cells.

Since the flies in my experiments were exposed to the nickel nanomaterials through dietary uptake, the primary exposure site is larval gastrointestinal tract. Among the different regions of foregut, midgut, and hindgut, midgut is the major site of digestion and nutrient uptake and shares many similarities with human small intestine (Apidianakis and Rahme, 2011). To test the hypothesis that nickel-based nanomaterials induce abnormal morphological changes to the midgut of *Drosophila melanogaster* larvae, I examined the general cellular structure of the midgut using confocal microscopy and two dyes: DAPI to examine the distribution of the nuclei and Alex488 phalloidin to examine the overall shape and structure of the cells. No distinct changes in gut morphology were detected and there was no evidence of leaking or ruptures (Figure 12).

To determine whether the cells within the midgut were killed due to nickel nanomaterial exposure, I stained living larval midguts with acridine orange and propidium iodide. Acridine orange(AO) is a vital dye that labels all living cells, whereas propidium iodide(PI) is cell impermeant and only labels dead or dying cells (Liu et al., 2015). As with the previous experiment, I observed no change in the number of propidium iodide staining cells in larval midgut from those larvae fed nickel nanoparticle diet when compared to the control groups or other experimental groups. However, I did observe that a large proportion of the gastrointestinal microbiota in the midgut was labeled with PI in nickel nanoparticle feed larvae when compared to the control and other experimental groups (Figure 13). *D. melanogaster* larvae and adults midguts harbor a broad range of microorganisms including bacteria and yeast (Olcott et al., 2010) and reduction of *Drosophila melanogaster* midgut microbiome can negatively modulate host

development (Shin et al., 2011). These results may partially explain some of the developmental delays that I have observed in larvae fed metallic nickel nanoparticle diets.

4.3.4 Hsp-70 and Oxidative Stress

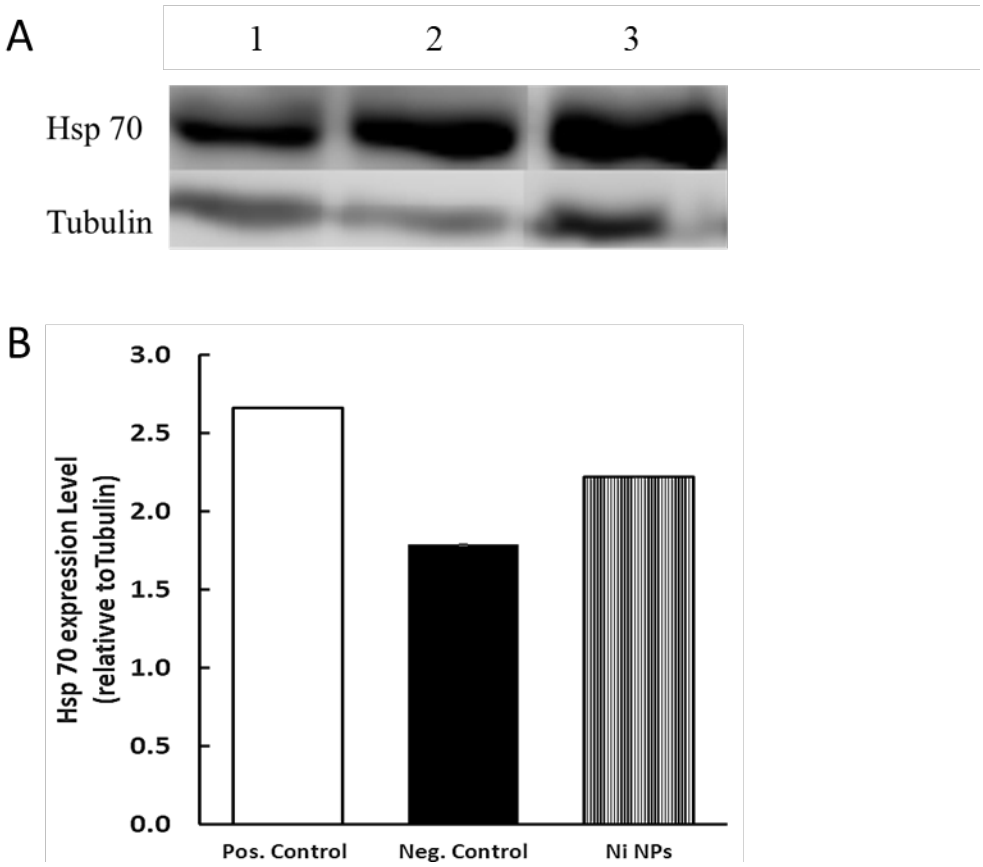

Figure 14. Western Blot Showing Hsp 70 Expression in *D. melanogaster* Larva after 5 Days Oral Exposure to Nickel Nanoparticles Containing Food. A) The lanes 1-3 are as follows: lane 1 no treatment (negative control); lane 2 positive control of Hsp 70; lane 3 nickel nanoparticles. B) Quantification of band intensity after relative to tubulin using ImageJ.

To determine whether a nickel nanoparticle diet induces a cellular stress response, I examined two stress indicators, Hsp70 and reactive oxygen species (ROS) as these responses may also serve as the basis for the underlying mechanisms of causing decrease viability and developmental delay. Heat shock proteins are highly conserved chaperones which response to acute heat and oxidative stress. As the major heat shock protein, Hsp70 is found in all organisms and refold misfolded proteins and also to eliminate irreversibly damaged proteins (Schlesinger, 1990). Generally, Hsp70 will help cells protect themselves from the environment, or metabolic stress such as the stress of a nanoparticle diet. In our evaluations of nickel nanoparticle-induced toxicity, larvae fed nickel nanoparticle diet exhibit an increase in the expression of Hsp70 (Figure 14), indicating that *Drosophila* larvae were under biological stress and possibly in response to oxidative stress.

Oxidative stress is the most reported mechanisms underlying nanotoxicity (Chifiriuc et al., 2016). Oxidative stress is generated when reactive oxygen species (ROS) exceed the intracellular balance and result in the subsequent damage to lipids, proteins, and DNA. To test for the generation of ROS within the midguts of larvae fed nickel nanomaterial diets, I used DHE to detect superoxide and hydrogen peroxide (Wang et al., 2013). DHE can freely permeate cell membranes and specifically detects superoxide production. Once oxidized by superoxide, DHE forms red fluorescent ethidium and interacts with DNA. Larvae fed nickel nanoparticle diet exhibited an increase in the expression of ROS (Figure 15). In the control groups, only basal amounts of ROS were detected, which is considered as a minimum threshold. This finding suggests that oral

ingestion of a diet containing nickel nanoparticles will induce oxidative stress, which may lead to decrease viability and extension of pupariation development.

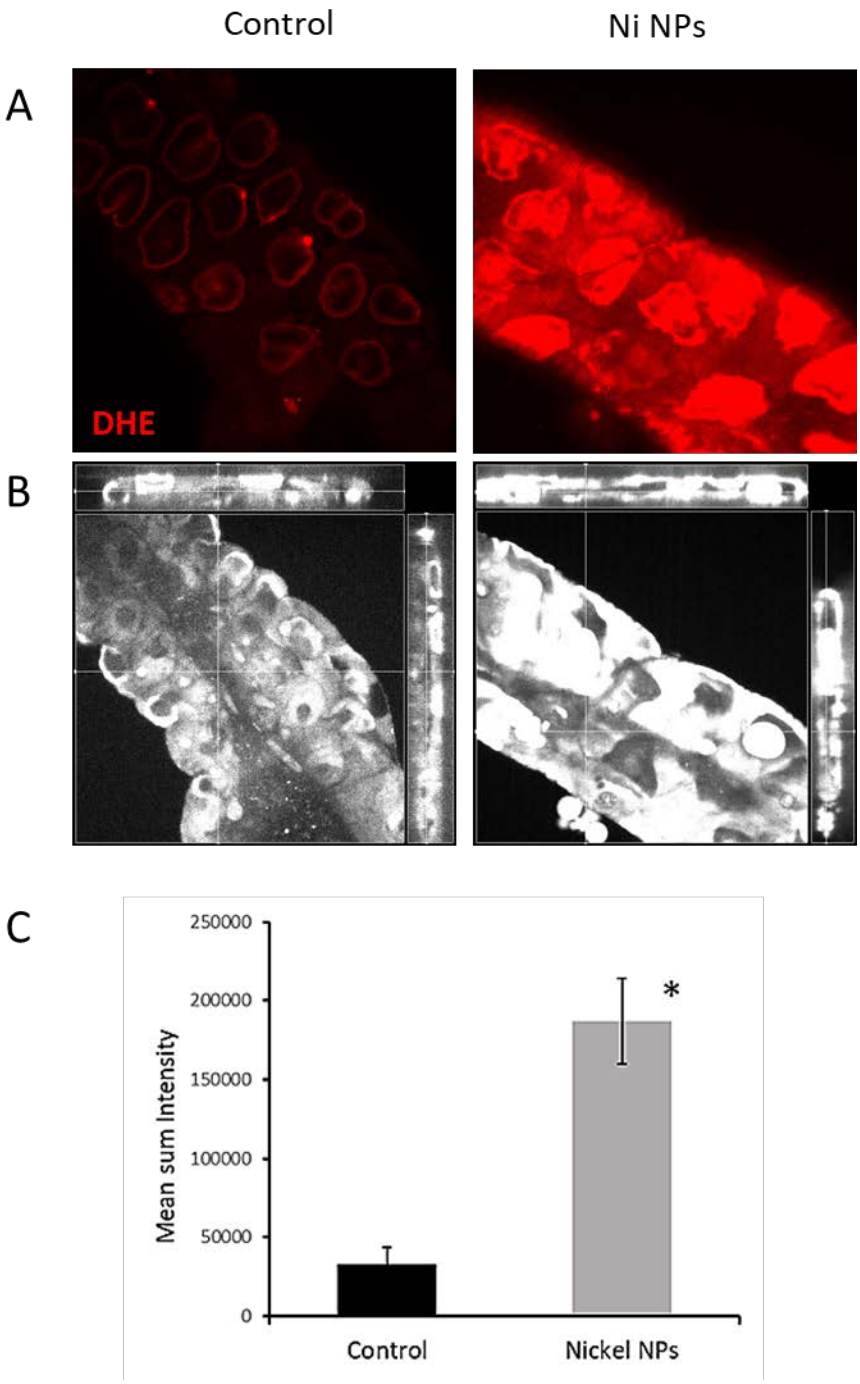

Figure 15. Nickel Nanoparticles Induce ROS in the Midgut of *D. melanogaster* Larvae. DHE staining in the control diet shows the basal level of ROS. Nickel/Ni nanoparticles (NPs) diet increased ROS generation. A) Slice views of midguts. B) Cutviews centered

on lumen region of midguts in black and white color that transferred from red staining ROS images. C) Intensity quantification of DHE staining ROS in fly midguts.

4.4 Conclusions

In conclusion, a nickel nanoparticles diet decreased viability and causes a developmental delay in pupariation. The subsequent loss of gut microbiome was detected. The observed effects can be explained by the overexpression of Hsp-70 and the oxidative stress by Ni NPs exposure. This study demonstrated the value of *D. melanogaster* in nanotoxicity studies to assess related mechanisms of metallic and metal oxide NPs.

Considering that both expressions of Hsp-70 and generation of ROS were detected after oral ingestion of nickel nanoparticles in *D. melanogaster*, further investigation is expected to focus on oxidative stress-related pathways. As a direction for future analysis, I hypothesize upregulations of Hypoxia-inducible factor -1 (HIF-1) and Metallothioneins (MTs) in nickel nanoparticle treated larvae. HIF-1 is an oxygen-sensitive transcription factor that is responsible for activating a series of genes adapted to low oxygen condition in organisms, which is also correlated with expression of MTs (Semenza, 1998).

CHAPTER V

MINERAL DEPOSITION AFTER NICKEL NANOPARTICLE INGESTION IN *DROSOPHILA MELANOGASTER*

5.1 Introduction

Biomineralization is a widespread process that occurs throughout development such as during bone formation and in the formation of carbonate structures (e.g. shells) in the invertebrates (Crenshaw, 1982; Olszta et al., 2007). In contrast, ectopic calcification refers to an inappropriate deposition of calcium compounds in soft tissue, which is commonly observed as a result of aging, disease, and injury (Giachelli, 1999). Kidney stone disease, also known as urolithiasis, is affecting up to 15% of the global population with the deposition of a broad range of calcium salts, uric acid, cysteine, and struvite (Barnela et al., 2012).

Depositions of calcium carbonate or calcite have been reported in a variety of organisms, including sea urchins, invertebrates, bacteria, and humans. Embryonic sea urchins form calcite spicules that are distributed throughout the organism in aggregates of 20 nm – 30 nm nanospheres (Vidavsky et al., 2014). Invertebrates form composites of calcium carbonate and chitin to produce tougher and less brittle cuticles (Suzuki, 2010). Nanobacteria in human serum can precipitate amorphous calcium carbonate in human blood (Martel and Young, 2008), can their presence is associated with a high risk for the development of kidney stones. Additionally, calcite microcrystals were found in human

brain and inner ear (Baconnier et al., 2002). In all of these cases, the mechanisms of calcification are poorly understood which limit the preventive and therapeutic measures against them.

In mammalian organisms, waste products in the blood represent primarily metabolic breakdown products, which cannot be further utilized. The major site of filteration, reabsorption, secretion and excretion of these waste products are the kidneys, which also regulate homeostasis, balance minerals, and produce hormones (Guyton, 1991). In *Drosophila melanogaster*, the excretion of metabolic wastes is performed by a tissue called the Malpighian tubules. Malpighian tubules are the insect renal tubule system, which works as kidneys to perform not only the transportation of Na^+/K^+ and organic solutes but also the excretion of calcium, uric acid, and phosphorus (Dow and Romero, 2010). Similar to the mammalian kidney, Malpighian tubules can recover from injury and regenerate through the differentiation of pluripotent stem cells (Singh et al., 2007). Recently, *D. melanogaster* has been used as *in vivo* model organisms for urolithiasis studies, considering the formation of calcium oxalate crystals induced by ethylene glycol (Chen et al., 2011). In this chapter, I show that a diet containing metallic nickel nanoparticles induces the formation of crystalline calcium mineral depositions in the Malpighian tubules within 5-7 days in *D. melanogaster* larvae. The formed crystals exhibit a broad range of fluorescent excitation and emission, and a chemical composition of calcium, carbon, and oxide with a ratio of 1:1:3.

5.2 Materials and Methods

5.2.1 Malpighian Tubule Dissection

D. melanogaster larvae were raised as described in CHAPTER IV. After 5 to 7 days of exposure to food containing 1mg/ml of nickel nanoparticles, larval tissue was dissected in 1X PBS under a Leica dissection light microscope using antimagnetic WPI Swiss Tweezers (World Precision Instruments, FL, USA).

5.2.2 Brightfield and Confocal Microscopy

To visualize the natural color and shape of depositing crystals, dissected Malpighian tubules were mounted on a glass slide with mounting media and examined under brightfield using a ZEISS Axio Imager 2. Fluorescent images were collected using a ZEISS Z1 spinning disc confocal microscope.

5.2.3 Electron Microscopy and Energy-Dispersive Spectroscopy (EDS) Microanalysis

Dissected larval tissue was transferred from 1X PBS into a droplet of pure water on the clean wafer. Malpighian tubules were gently extended and dried out at room temperature. A thin layers of 3 nm gold-pallidum was coated on the surface of the sample. SEM images were obtained as described in CHAPTER III and energy dispersive X-ray analysis was performed at a voltage of 15 KeV.

5.3 Results and Discussion

5.3.1 Formation of Fluorescent Crystals in Malpighian Tubules

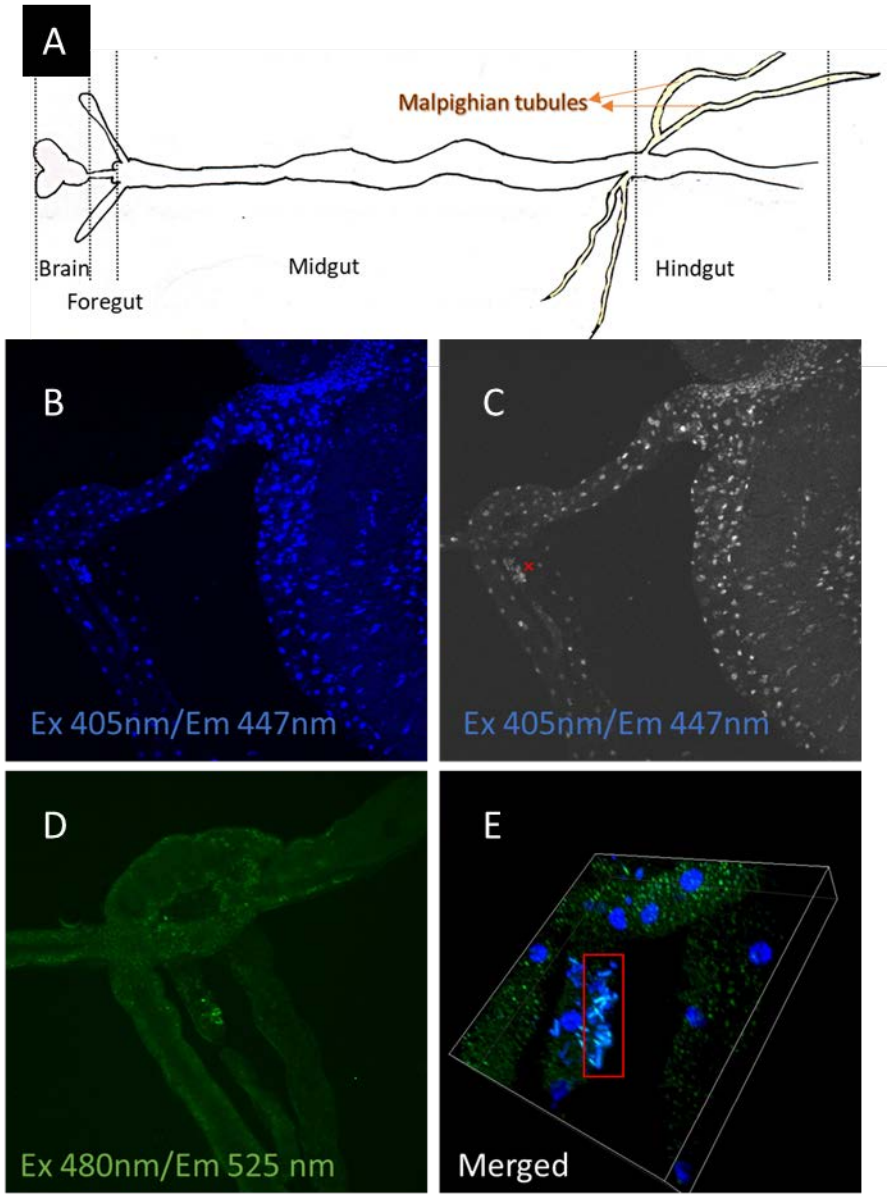

Figure 16. Ingestion of Nickel Nanoparticles Induces Fluorescent Crystal Formation in Malpighian Tubules of *D. melanogaster* Larvae. A) A schematic illustration of the fruit fly gut. The yellow region indicates the Malpighian tubule. B, C) Samples were excited by 405 nm laser and imaged under the DAPI channel. C) X marked the location of

crystals in the Malpighian tubule. D) Excitation at 480nm (FITC) laser E) Redbox labels crystal in merging of DAPI and FITC channel. Tissue nuclei were stained with DAPI.

During the confocal examinations of different regions of *D. melanogaster* larval tissue, including brain, foregut, midgut, Malpighian tubule, fat body, and hindgut (Figure 16A), auto-fluorescent crystals were located in Malpighian tubule after 5 - 7 days' exposure of nickel nanoparticle food (Figure 16). While no crystal formation was detected in larvae fed a normal cornmeal-yeast medium diet (Figure 17), dietary uptake of nickel nanoparticles induced biomineralization of crystals in *Drosophila* Malpighian tubules of third instar larvae. The detected crystals possess a broad range of excitation wavelengths, which can be observed after excitation with both a 405nm laser and a 480nm laser (Figure 16 B-E).

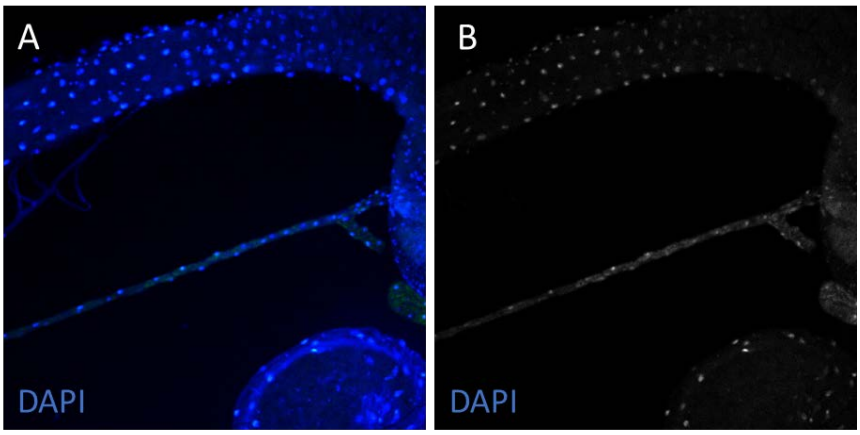

Figure 17. No Crystal Formation Was Found in Larvae Feed a Normal Diet. Midgut tissue nuclei were stained with the fluorescent dye DAPI.

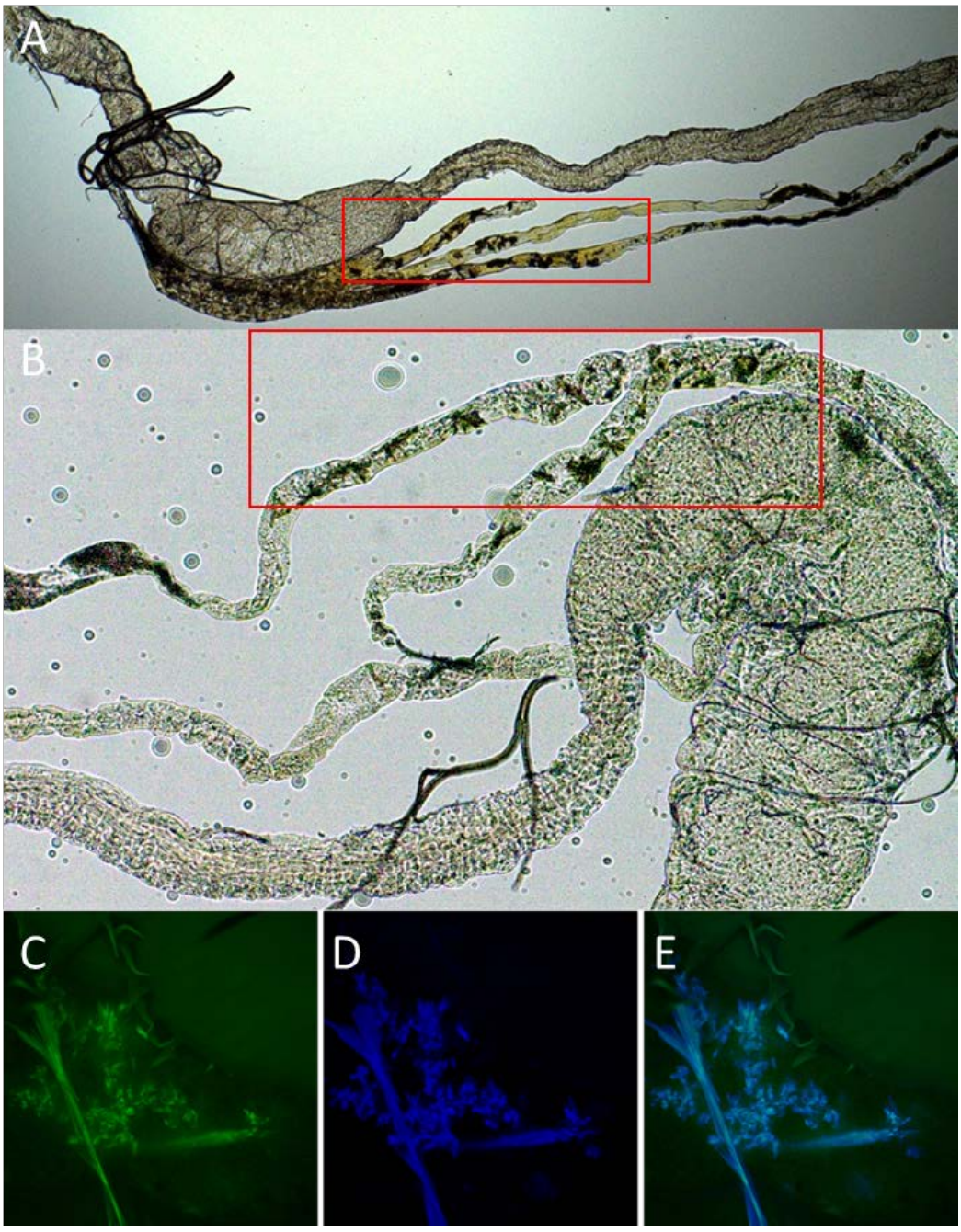

Figure 18. Dietary Uptake of Nickel Nanoparticles Induced Multiple Crystals Deposition in Malpighian Tubules. A, B) Brightfield microscopy images reveal multiple depositions of green crystals in Malpighian tubules under natural bright light with magnifications of 50x and 100x. C, D, E) Total magnification of 630x under filters of DAPI, FITC, and both.

The crystal depositions in Malpighian tubules were also visible under brightfield microscopy (Figure 18 A, B), which exhibit as green color crystals. The crystals have a range of sizes with the maximum width of 30 - 60 μm and their size appear to be limited by the width of the Malpighian tubule. Higher magnification confocal images further confirmed the presence and shape of the crystal depositions in the larval Malpighian tubules that were induced by the nickel nanoparticle diet (Figure 18 C-E). Interestingly, the emission of green fluorescence from the crystals is more concentrated in the core region, while the blue fluorescent emission covers most of the regions of formed crystals (Figure 18 C and D); this variation in the fluorescence is unusual for a fluorescent material and suggests some chemical or structural diversity within the deposited material itself (Wolf, 2013). There are a number of different fluorescent minerals occurring naturally in living systems (Robbins, 2013). Deep-sea corals emit fluorescent light from different pigments (Mazel, 1997). A more detailed chemical and structural analysis of the fluorescent crystals found in the Malpighian tubules of *Drosophila melanogaster* larvae fed by nickel nanoparticles is required to better understand the nature of their fluorescent properties.

5.3.2 Identification of Depositing Crystals Induced by Nickel Nanoparticle Ingestion

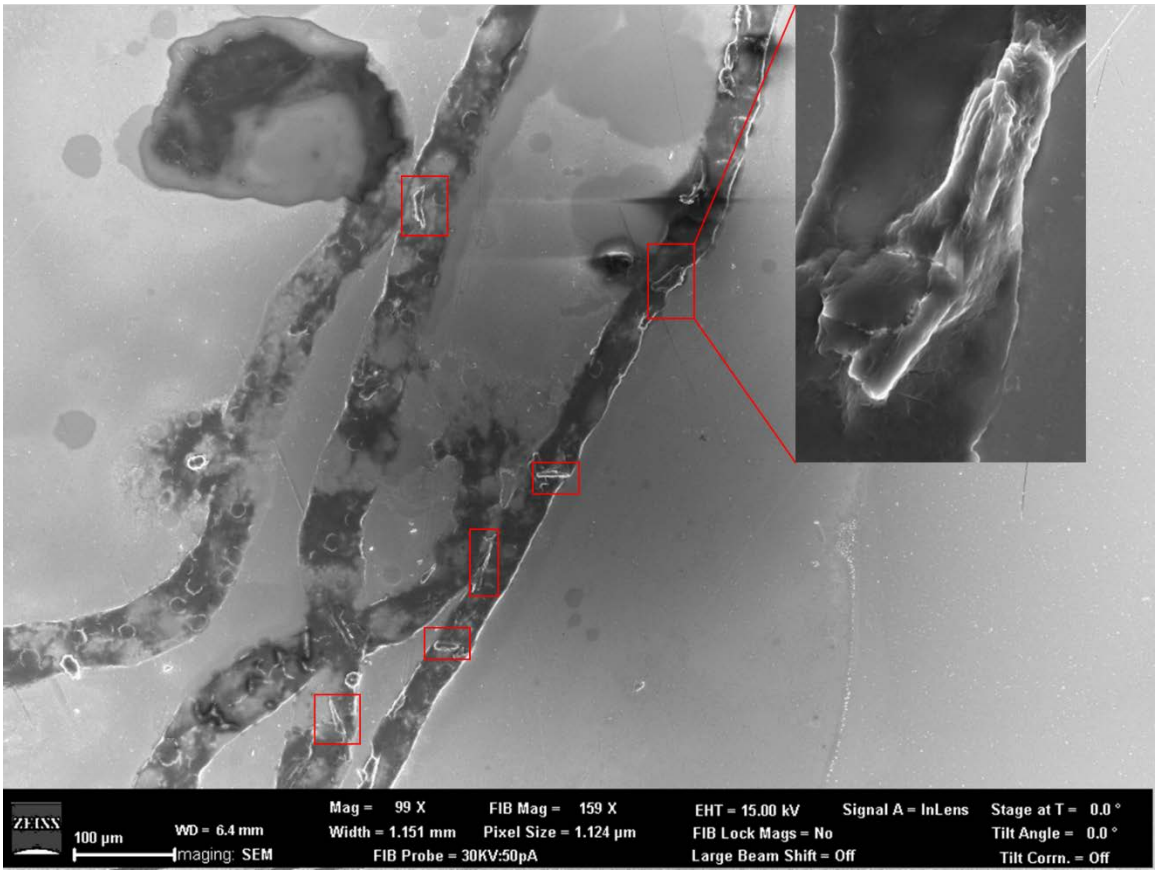

Figure 19. Images of Scanning Electron Microscopy Reveal the Presence of Crystals in a Dry Sample of the Malpighian Tubules. Multiple crystals were located in the tissue (red boxes).

To obtain the chemical composition of depositing crystals in Malpighian tubule, I performed a detailed scanning electron microscopy (SEM) and energy-dispersive X-ray (EDX) spectroscopy analysis. EDX analysis measures the energy and intensity distribution of the characteristic X-rays produced after a specimen is interrogated by a primary electron beam (Srnová-Šloufová et al., 2004). After dissecting in 1X PBS, I transferred the Malpighian tubules from larvae fed a nickel nanoparticle diet onto a silicon wafer and added one drop (~10 µl) of pure water. Cells of Malpighian tubule contain abundant ion channels (Na+, K+, Cl-), hence the addition of water will disrupt the iso-osmotic state of the tissue and speed up fluid excretion (Dow et al., 1994). As the water droplet was quickly drying, some of the crystals and salts were excreted while some of the crystals remained inside the Malpighian tubule (Figure 19).

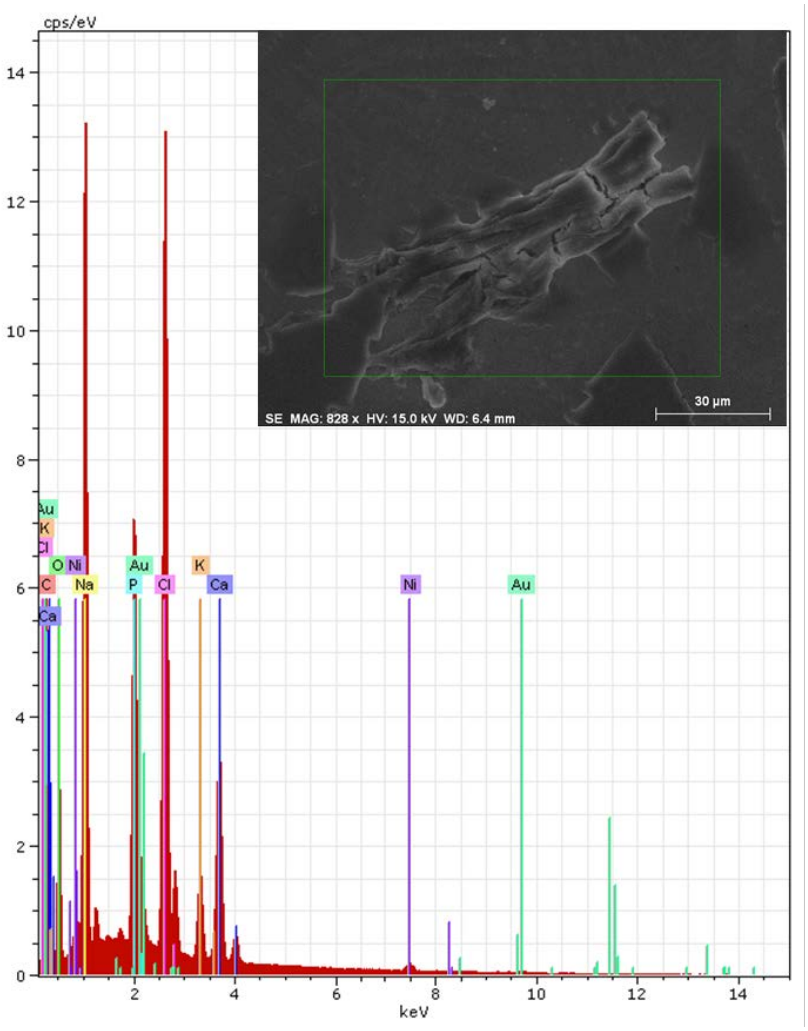

Figure 20. Mapping of Energy-Dispersive X-Ray Spectroscopy Microanalysis. All peaks detected from mapping results were labeled in the spectrum.

Once I located an excreted crystal, I mapped its elemental composition with SEM-EDX. The EDX spectrum of the nickel nanoparticle-induced crystal indicated that several metallic and salt elements were represented. Five elements demonstrated clear mapping patterns (Figure 21) above the background noise, which had no detectable pattern. The elements carbon, oxygen, and calcium were found in the crystal, while sodium and chloride deposited from the saline dissection buffer on the surface of the crystal (Figure 21).

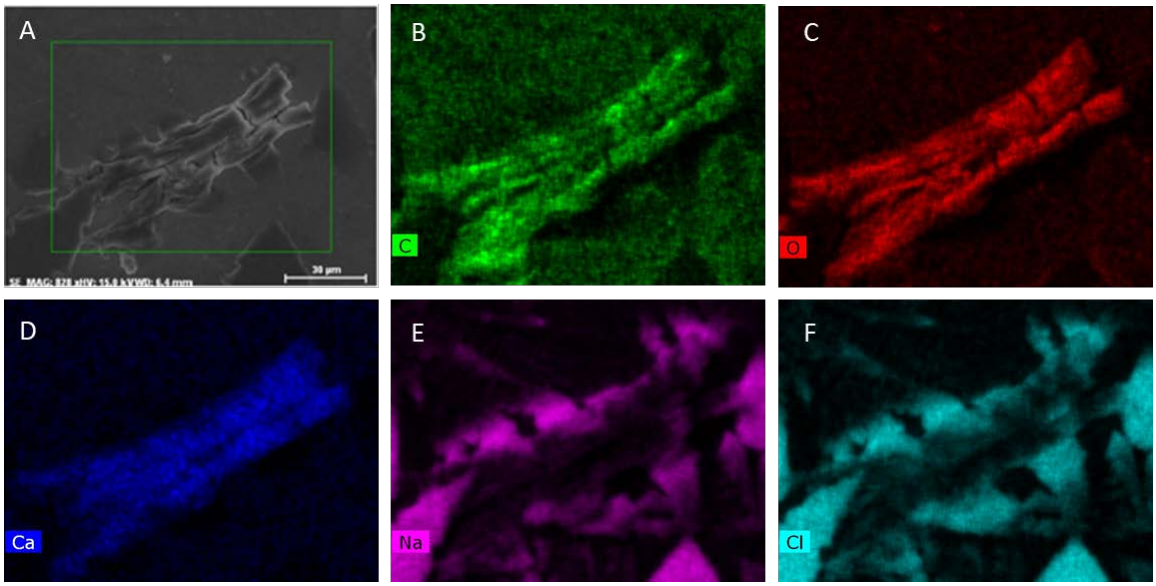

Figure 21. Mapping of Energy-Dispersive X-Ray Spectroscopy Microanalysis. A) Mapping region is circled by a green box. B-D) Element contents of the crystal were narrowed down to carbon, oxide, and calcium. E, F) Sodium and chloride were found to exist in the surrounding salts around the crystal.

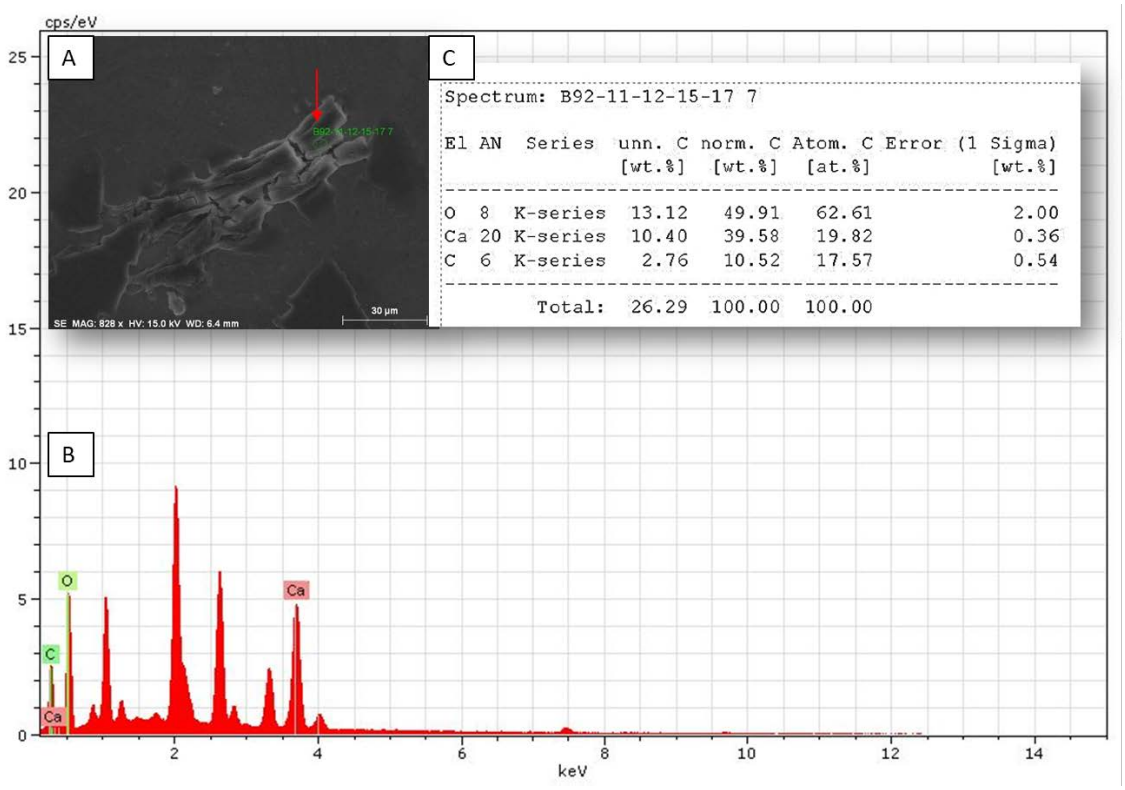

Figure 22. Point Analysis and Elemental Quantification of the Spectrum of Depositing Crystal. A) Arrow points to the location of point analysis. B) The spectrum obtained from point analysis. C) Quantification analysis based on the obtained spectrum.

To determine the chemical formula of depositing crystals, I performed an additional qualitative analysis using EDX on the spectrum information (Figure 22). The atom concentrations of predominate components of these nickel nanoparticle-induced crystals were found to be 62.61% of oxygen, 19.82% of calcium, and 17.57% of carbon. The results of SEM-EDX microanalysis confirmed that the crystal composition has a predominate chemical formula of $CaCO_3$. Although the crystalline structure needs further confirmation using TEM and electron diffraction, the fluorescent nature of these depositions, their green color, and their elemental composition strongly suggest that the crystal depositions are either calcite or aragonite. Future work on their crystallinity should lead to determination of the crystal type as calcite is trigonal and aragonite is orthorhombic (Tong et al., 2004).

The function of mammalian kidney or *Drosophila*'s Malpighian tubule is to eliminate nitrogenous waste and toxins (Dow et al., 1994; Guyton, 1991). In human kidneys, the renal stone formation is considered as ectopic calcification with risk factors such as dehydration and high dietary of oxalate (Barnela et al., 2012). In *D. melanogaster*, ectopic calcification was also reported by Chen et al., in which formation of calcium oxalate in Malpighian tubule was induced using ethylene glycol, sodium oxalate, or hydroxyl-L-proline (Chen et al., 2011). Chemically, even though their SEM-EDX analysis also indicated the presence of carbon, calcium, and oxide, both the element ratio and crystal shape were different from ours, suggesting that different mechanisms might be involved for ectopic calcification in *Drosophila* Malpighian tubule due to a diet containing nickel nanoparticles. In another study of *Drosophila* ectopic calcification,

knockdown of xanthine dehydrogenase resulted in dramatic increase of tubule concretion formation, which can be prevented by blocking zinc transporters (Chi et al., 2015). The finding of Chi el al., indicates that the important role of zinc ion transporters on the mineralization in the Malpighian tubule. Other ion channels were also reported to affect calcium mineralization. Calcium channels were shown to be involved in ectopic calcification in aquatic plants (Volk et al., 2004).

5.4 Conclusion

Oral ingestion of nickel nanoparticles induced the mineral deposition in Malpighian tubules in the larvae of *Drosophila melanogaster*. The depositions are unique and consist of green mineral crystals that exhibit a wide range of fluorescence and a chemical composition determined to be calcium carbonate. Future investigations will confirm the crystal structure and the exact nature of these mineral depositions. Future studies will also evaluate the potential roles that calcium ion channels may play in the formation of these mineral crystals and the effects nickel nanomaterials have on these channels. Finally, elucidation of the underlying mechanisms of inducing mineral deposition by nickel nanoparticles is essential for nickel nanoparticle risk management and safe handling protocols.

REFERENCE LIST

Abbott Chalew, T.E., Schwab, K.J., 2013. Toxicity of commercially available engineered nanoparticles to Caco-2 and SW480 human intestinal epithelial cells. Cell biology and toxicology 29, 101-116.

Abramenko, N.B., Demidova, T.B., Abkhalimov capital Ie, C., Ershov, B.G., Krysanov, E.Y., Kustov, L.M., 2018. Ecotoxicity of different-shaped silver nanoparticles: Case of zebrafish embryos. J Hazard Mater 347, 89-94.

Ahamed, M., 2011. Toxic response of nickel nanoparticles in human lung epithelial A549 cells. Toxicology in Vitro 25, 930-936.

Akbarzadeh, A., Rezaei-Sadabady, R., Davaran, S., Joo, S.W., Zarghami, N., Hanifehpour, Y., Samiei, M., Kouhi, M., Nejati-Koshki, K., 2013. Liposome: classification, preparation, and applications. Nanoscale Research Letters 8, 102-102.

Alkilany, A.M., Nagaria, P.K., Hexel, C.R., Shaw, T.J., Murphy, C.J., Wyatt, M.D., 2009. Cellular uptake and cytotoxicity of gold nanorods: molecular origin of cytotoxicity and surface effects. Small 5, 701-708.

Almeida, J.P., Chen, A.L., Foster, A., Drezek, R., 2011. In vivo biodistribution of nanoparticles. Nanomedicine (London, England) 6, 815-835.

Amini, S.M., Gilaki, M., Karchani, M., 2014. Safety of Nanotechnology in Food Industries. Electronic Physician 6, 962-968.

Apidianakis, Y., Rahme, L.G., 2011. Drosophila melanogaster as a model for human intestinal infection and pathology. Disease Models & Mechanisms 4, 21-30.

Armand, L., Dagouassat, M., Belade, E., Simon-Deckers, A., Le Gouvello, S., Tharabat, C., Duprez, C., Andujar, P., Pairon, J.C., Boczkowski, J., Lanone, S., 2013. Titanium dioxide nanoparticles induce matrix metalloprotease 1 in human pulmonary fibroblasts partly via an interleukin-1beta-dependent mechanism. Am J Respir Cell Mol Biol 48, 354-363.

Baan, R., Straif, K., Grosse, Y., Secretan, B., El Ghissassi, F., Cogliano, V., 2006. Carcinogenicity of carbon black, titanium dioxide, and talc. The Lancet Oncology 7, 295-296.

Baconnier, S., Lang, S.B., Polomska, M., Hilczer, B., Berkovic, G., Meshulam, G., 2002. Calcite microcrystals in the pineal gland of the human brain: first physical and chemical studies. Bioelectromagnetics 23, 488-495.Bahamonde, J., Brenseke, B., Chan, M.Y., Kent, R.D., Vikesland, P.J., Prater, M.R., 2018. Gold Nanoparticle Toxicity in Mice and Rats: Species Differences. Toxicologic pathology, 192623318770608.

Ballottin, D., Fulaz, S., Cabrini, F., Tsukamoto, J., Durán, N., Alves, O.L., Tasic, L., 2017. Antimicrobial textiles: Biogenic silver nanoparticles against Candida and Xanthomonas. Materials Science and Engineering: C 75, 582-589.

Barnela, S.R., Soni, S.S., Saboo, S.S., Bhansali, A.S., 2012. Medical management of renal stone. Indian Journal of Endocrinology and Metabolism 16, 236-239.

Baun, A., Hartmann, N.B., Grieger, K., Kusk, K.O., 2008. Ecotoxicity of engineered nanoparticles to aquatic invertebrates: a brief review and recommendations for future toxicity testing. Ecotoxicology (London, England) 17, 387-395.

Benn, T.M., Westerhoff, P., Herckes, P., 2011. Detection of fullerenes (C(60) and C(70)) in commercial cosmetics. Environmental pollution (Barking, Essex : 1987) 159, 1334-1342.

Bergin, I.L., Witzmann, F.A., 2013. Nanoparticle toxicity by the gastrointestinal route: evidence and knowledge gaps. Int J Biomed Nanosci Nanotechnol 3.

Bertrand, N., Grenier, P., Mahmoudi, M., Lima, E.M., Appel, E.A., Dormont, F., Lim, J.-M., Karnik, R., Langer, R., Farokhzad, O.C., 2017. Mechanistic understanding of in vivo protein corona formation on polymeric nanoparticles and impact on pharmacokinetics. Nature Communications 8, 777.

Bhattacharjee, S., 2016. DLS and zeta potential – What they are and what they are not? Journal of Controlled Release 235, 337-351.

Bhattacharya, R., Mukherjee, P., 2008. Biological properties of “naked” metal nanoparticles. Advanced Drug Delivery Reviews 60, 1289-1306.

Braakhuis, H.M., Gosens, I., Krystek, P., Boere, J.A., Cassee, F.R., Fokkens, P.H., Post, J.A., van Loveren, H., Park, M.V., 2014. Particle size dependent deposition and pulmonary inflammation after short-term inhalation of silver nanoparticles. Particle and fibre toxicology 11, 49.

Bundschuh, M., Filser, J., Luderwald, S., McKee, M.S., Metreveli, G., Schaumann, G.E., Schulz, R., Wagner, S., 2018. Nanoparticles in the environment: where do we come from, where do we go to? Environmental sciences Europe 30, 6.

Buzea, C., Pacheco, I.I., Robbie, K., 2007. Nanomaterials and nanoparticles: Sources and toxicity. Biointerphases 2, MR17-MR71.

Cabuzu, D., Cirja, A., Puiu, R., Grumezescu, A.M., 2015. Biomedical applications of gold nanoparticles. Current topics in medicinal chemistry 15, 1605-1613.

Campelo, J.M., Luna, D., Luque, R., Marinas, J.M., Romero, A.A., 2009. Sustainable preparation of supported metal nanoparticles and their applications in catalysis. ChemSusChem 2, 18-45.

Capek, I., 2017. Noble metal nanoparticles : preparation, composite nanostructures, biodecoration and collective properties.

Carmona, E.R., Escobar, B., Vales, G., Marcos, R., 2015a. Genotoxic testing of titanium dioxide anatase nanoparticles using the wing-spot test and the comet assay in Drosophila. Mutation Research/Genetic Toxicology and Environmental Mutagenesis 778, 12-21.

Carmona, E.R., Inostroza-Blancheteau, C., Obando, V., Rubio, L., Marcos, R., 2015b. Genotoxicity of copper oxide nanoparticles in Drosophila melanogaster. Mutation research. Genetic toxicology and environmental mutagenesis 791, 1-11.

Chairuangkitti, P., Lawanprasert, S., Roytrakul, S., Aueviriyavit, S., Phummiratch, D., Kulthong, K., Chanvorachote, P., Maniratanachote, R., 2013. Silver nanoparticles induce toxicity in A549 cells via ROS-dependent and ROS-independent pathways. Toxicol In Vitro 27.

Charitidis, C.A., Georgiou, P., Koklioti, M.A., Trompeta, A.-F., Markakis, V., 2014. Manufacturing nanomaterials: from research to industry. Manufacturing Rev. 1, 11.

Chen, Y.-H., Liu, H.-P., Chen, H.-Y., Tsai, F.-J., Chang, C.-H., Lee, Y.-J., Lin, W.-Y., Chen, W.-C., 2011. Ethylene glycol induces calcium oxalate crystal deposition in Malpighian tubules: a Drosophila model for nephrolithiasis/urolithiasis. Kidney International 80, 369-377.

Chi, T., Kim, M.S., Lang, S., Bose, N., Kahn, A., Flechner, L., Blaschko, S.D., Zee, T., Muteliefu, G., Bond, N., Kolipinski, M., Fakra, S.C., Mandel, N., Miller, J., Ramanathan, A., Killilea, D.W., Brückner, K., Kapahi, P., Stoller, M.L., 2015. A Drosophila Model Identifies a Critical Role for Zinc in Mineralization for Kidney Stone Disease. PLOS ONE 10, e0124150.

Chifiriuc, M.C., Ratiu, A.C., Popa, M., Ecovoiu, A.A., 2016. Drosophotoxicology: An Emerging Research Area for Assessing Nanoparticles Interaction with Living Organisms. Int J Mol Sci 17, 36.

Choi, J., Reipa, V., Hitchins, V.M., Goering, P.L., Malinauskas, R.A., 2011. Physicochemical characterization and in vitro hemolysis evaluation of silver nanoparticles. Toxicol Sci 123, 133-143.

Chow, E.K., Ho, D., 2013. Cancer nanomedicine: from drug delivery to imaging. Science translational medicine 5, 216rv214.

Clemente, Z., Castro, V.L., Moura, M.A., Jonsson, C.M., Fraceto, L.F., 2014. Toxicity assessment of TiO(2) nanoparticles in zebrafish embryos under different exposure conditions. Aquatic toxicology (Amsterdam, Netherlands) 147, 129-139.

Comfort, K.K., Maurer, E.I., Braydich-Stolle, L.K., Hussain, S.M., 2011. Interference of silver, gold, and iron oxide nanoparticles on epidermal growth factor signal transduction in epithelial cells. ACS Nano 5.

Crenshaw, M.A., 1982. Mechanisms of Normal Biological Mineralization of Calcium Carbonates. Springer Berlin Heidelberg, Berlin, Heidelberg, pp. 243-257.

De Volder, M.F.L., Tawfick, S.H., Baughman, R.H., Hart, A.J., 2013. Carbon Nanotubes: Present and Future Commercial Applications. Science (New York, N.Y.) 339, 535-539.

Dhand, C., Dwivedi, N., Loh, X.J., Jie Ying, A.N., Verma, N.K., Beuerman, R.W., Lakshminarayanan, R., Ramakrishna, S., 2015. Methods and strategies for the synthesis of diverse nanoparticles and their applications: a comprehensive overview. RSC Advances 5, 105003-105037.

Dhawan, A., Sharma, V., 2010. Toxicity assessment of nanomaterials: methods and challenges. Anal Bioanal Chem 398, 589-605.

Dizaj, S.M., Lotfipour, F., Barzegar-Jalali, M., Zarrintan, M.H., Adibkia, K., 2014. Antimicrobial activity of the metals and metal oxide nanoparticles. Materials science & engineering. C, Materials for biological applications 44, 278-284.

Dohnalova, K., Gregorkiewicz, T., Kusova, K., 2014. Silicon quantum dots: surface matters. Journal of physics. Condensed matter : an Institute of Physics journal 26, 173201.

Donaldson, K., Stone, V., Tran, C.L., Kreyling, W., Borm, P.J., 2004. Nanotoxicology. Occup Environ Med 61, 727-728.

Doustan, F., Pasha, M.A., 2016. Growth of carbon nanotubes over Fe-Co and Ni-Co catalysts supported on different phases of TiO2 substrate by thermal CVD. Fullerenes, Nanotubes and Carbon Nanostructures 24, 25-33.

Dow, J.A., Maddrell, S.H., Gortz, A., Skaer, N.J., Brogan, S., Kaiser, K., 1994. The malpighian tubules of Drosophila melanogaster: a novel phenotype for studies of fluid secretion and its control. The Journal of experimental biology 197, 421-428.

Dow, J.A., Romero, M.F., 2010. Drosophila provides rapid modeling of renal development, function, and disease. American journal of physiology. Renal physiology 299, F1237-1244.

Dumala, N., Mangalampalli, B., Kalyan Kamal, S.S., Grover, P., 2018. Biochemical alterations induced by nickel oxide nanoparticles in female Wistar albino rats after acute oral exposure. Biomarkers 23, 33-43.

Dziendzikowska, K., Gromadzka-Ostrowska, J., Lankoff, A., Oczkowski, M., Krawczynska, A., Chwastowska, J., Sadowska-Bratek, M., Chajduk, E., Wojewodzka, M., Dusinska, M., Kruszewski, M., 2012. Time-dependent biodistribution and excretion of silver nanoparticles in male Wistar rats. J Appl Toxicol 32, 920-928.

El Badawy, A.M., Silva, R.G., Morris, B., Scheckel, K.G., Suidan, M.T., Tolaymat, T.M., 2011. Surface charge-dependent toxicity of silver nanoparticles. Environmental Science and Technology 45, 283-287.

Elgrabli, D., Beaudouin, R., Jbilou, N., Floriani, M., Pery, A., Rogerieux, F., Lacroix, G., 2015. Biodistribution and Clearance of TiO2 Nanoparticles in Rats after Intravenous Injection. PLoS One 10, e0124490.

Fabian, E., Landsiedel, R., Ma-Hock, L., Wiench, K., Wohlleben, W., van Ravenzwaay, B., 2008. Tissue distribution and toxicity of intravenously administered titanium dioxide nanoparticles in rats. Archives of toxicology 82, 151-157.

Faraday, M., 1857. X. The Bakerian Lecture. —Experimental relations of gold (and other metals) to light. Philosophical Transactions of the Royal Society of London 147, 145-181.

Farkas, J., Christian, P., Gallego-Urrea, J.A., Roos, N., Hassellov, M., Tollefsen, K.E., Thomas, K.V., 2011. Uptake and effects of manufactured silver nanoparticles in rainbow trout (Oncorhynchus mykiss) gill cells. Aquatic toxicology (Amsterdam, Netherlands) 101, 117-125.

Featherstone, D.E., Chen, K., Broadie, K., 2009. Harvesting and Preparing Drosophila Embryos for Electrophysiological Recording and Other Procedures. Journal of Visualized Experiments : JoVE, 1347.

Florence, A.T., Hillery, A.M., Hussain, N., Jani, P.U., 1995. Factors Affecting the Oral Uptake and Translocation of Polystyrene Nanoparticles: Histological and Analytical Evidence. Journal of Drug Targeting 3, 65-70.

Foldbjerg, R., Dang, D.A., Autrup, H., 2011. Cytotoxicity and genotoxicity of silver nanoparticles in the human lung cancer cell line, A549. Archives of toxicology 85, 743-750.

Frohlich, E., 2012. The role of surface charge in cellular uptake and cytotoxicity of medical nanoparticles. International journal of nanomedicine 7, 5577-5591.

Ghobadian, M., Nabiuni, M., Parivar, K., Fathi, M., Pazooki, J., 2015. Toxic effects of magnesium oxide nanoparticles on early developmental and larval stages of zebrafish (Danio rerio). Ecotoxicology and environmental safety 122, 260-267.

Giachelli, C.M., 1999. Ectopic Calcification : Gathering Hard Facts about Soft Tissue Mineralization. The American journal of pathology 154, 671-675.

Gliga, A.R., Skoglund, S., Odnevall Wallinder, I., Fadeel, B., Karlsson, H.L., 2014a. Size-dependent cytotoxicity of silver nanoparticles in human lung cells: the role of cellular uptake, agglomeration and Ag release. Particle and Fibre Toxicology 11, 11.

Gliga, A.R., Skoglund, S., Wallinder, I.O., Fadeel, B., Karlsson, H.L., 2014b. Size-dependent cytotoxicity of silver nanoparticles in human lung cells: the role of cellular uptake, agglomeration and Ag release. Particle Fibre Toxicol 11.

Goldburg, W.I., 1999. Dynamic light scattering. American Journal of Physics 67, 1152-1160.

Gopinath, P., Gogoi, S.K., Sanpui, P., Paul, A., Chattopadhyay, A., Ghosh, S.S., 2010. Signaling gene cascade in silver nanoparticle induced apoptosis. Colloids Surf B Biointerfaces 77, 240-245.

Grassian, V.H., O'Shaughnessy, P.T., Adamcakova-Dodd, A., Pettibone, J.M., Thorne, P.S., 2007. Inhalation Exposure Study of Titanium Dioxide Nanoparticles with a Primary Particle Size of 2 to 5 nm. Environmental Health Perspectives 115, 397-402.

Guo, D., Wu, C., Hu, H., Wang, X., Li, X., Chen, B., 2009. Study on the enhanced cellular uptake effect of daunorubicin on leukemia cells mediated via functionalized nickel nanoparticles. Biomedical materials (Bristol, England) 4, 025013.

Guyton, A., 1991. Blood pressure control--special role of the kidneys and body fluids. Science 252, 1813-1816.

Hadrup, N., Lam, H.R., 2014. Oral toxicity of silver ions, silver nanoparticles and colloidal silver--a review. Regul Toxicol Pharmacol 68, 1-7.

Hahn, A., Fuhlrott, J., Loos, A., Barcikowski, S., 2012. Cytotoxicity and ion release of alloy nanoparticles. Journal of Nanoparticle Research 14, 686.

Han, J.W., Gurunathan, S., Jeong, J.-K., Choi, Y.-J., Kwon, D.-N., Park, J.-K., Kim, J.-H., 2014. Oxidative stress mediated cytotoxicity of biologically synthesized silver nanoparticles in human lung epithelial adenocarcinoma cell line. Nanoscale Research Letters 9, 459.

Hanagata, N., Zhuang, F., Connolly, S., Li, J., Ogawa, N., Xu, M., 2011. Molecular responses of human lung epithelial cells to the toxicity of copper oxide nanoparticles inferred from whole genome expression analysis. ACS Nano 5, 9326-9338.

Horie, M., Sugino, S., Kato, H., Tabei, Y., Nakamura, A., Yoshida, Y., 2016. Does photocatalytic activity of TiO2 nanoparticles correspond to photo-cytotoxicity? Cellular uptake of TiO2 nanoparticles is important in their photo-cytotoxicity. Toxicol Mech Methods 26, 284-294.

Hradil, J., Pisarev, A., Babič, M., Horák, D., 2007. Dextran-modified iron oxide nanoparticles. China Particuology 5, 162-168.

Hu, W., Culloty, S., Darmody, G., Lynch, S., Davenport, J., Ramirez-Garcia, S., Dawson, K.A., Lynch, I., Blasco, J., Sheehan, D., 2014. Toxicity of copper oxide nanoparticles in the blue mussel, Mytilus edulis: a redox proteomic investigation. Chemosphere 108, 289-299.

Hussain, S., Thomassen, L.C., Ferecatu, I., Borot, M.C., Andreau, K., Martens, J.A., Fleury, J., Baeza-Squiban, A., Marano, F., Boland, S., 2010. Carbon black and titanium dioxide nanoparticles elicit distinct apoptotic pathways in bronchial epithelial cells. Particle and fibre toxicology 7, 10.

Iavicoli, I., Leso, V., Bergamaschi, A., 2012. Toxicological effects of titanium dioxide nanoparticles: a review of in vivo studies. J. Nanomaterials 2012, 5-5.

Iversen, N.K., Frische, S., Thomsen, K., Laustsen, C., Pedersen, M., Hansen, P.B., Bie, P., Fresnais, J., Berret, J.F., Baatrup, E., Wang, T., 2013. Superparamagnetic iron oxide polyacrylic acid coated gamma-Fe2O3 nanoparticles do not affect kidney function but cause acute effect on the cardiovascular function in healthy mice. Toxicology and applied pharmacology 266, 276-288.

Jelinek, R., 2017. Carbon quantum dots : synthesis, properties and applications.

Jiang, W., Kim, B.Y.S., Rutka, J.T., Chan, W.C.W., 2008. Nanoparticle-mediated cellular response is size-dependent. Nature Nanotechnology 3, 145-150.

Jin, C.-Y., Zhu, B.-S., Wang, X.-F., Lu, Q.-H., 2008. Cytotoxicity of Titanium Dioxide Nanoparticles in Mouse Fibroblast Cells. Chemical Research in Toxicology 21, 1871-1877.

Jovin, T.M., 2003. Quantum dots finally come of age. Nature biotechnology 21, 32-33.

Kawata, K., Osawa, M., Okabe, S., 2009. In vitro toxicity of silver nanoparticles at noncytotoxic doses to HepG2 human hepatoma cells. Envir Sci Tech 43.

Kiss, B., Bíró, T., Czifra, G., Tóth, B.I., Kertész, Z., Szikszai, Z., Kiss, Á.Z., Juhász, I., Zouboulis, C.C., Hunyadi, J., 2008. Investigation of micronized titanium dioxide penetration in human skin xenografts and its effect on cellular functions of human skin-derived cells. Experimental Dermatology 17, 659-667.

Kokhanovsky, A.A., 2009. Light scattering reviews 4 : single light scattering and radiative transfer.

Kotov, Y.A., 2003. Electric Explosion of Wires as a Method for Preparation of Nanopowders. Journal of Nanoparticle Research 5, 539-550.

Kuempel, E.D., Tran, C.L., Castranova, V., Bailer, A.J., 2006. Lung dosimetry and risk assessment of nanoparticles: evaluating and extending current models in rats and humans. Inhal Toxicol 18, 717-724.

Kurlyandskaya, G.V., Bhagat, S.M., Safronov, A.P., Beketov, I.V., Larrañaga, A., 2011. Spherical magnetic nanoparticles fabricated by electric explosion of wire. AIP Advances 1, 042122.

Lankveld, D.P.K., Oomen, A.G., Krystek, P., Neigh, A., Troost – de Jong, A., Noorlander, C.W., Van Eijkeren, J.C.H., Geertsma, R.E., De Jong, W.H., 2010. The kinetics of the tissue distribution of silver nanoparticles of different sizes. Biomaterials 31, 8350-8361.

Larsen, S.T., Roursgaard, M., Jensen, K.A., Nielsen, G.D., 2010. Nano titanium dioxide particles promote allergic sensitization and lung inflammation in mice. Basic & clinical pharmacology & toxicology 106, 114-117.

Latvala, S., Hedberg, J., Di Bucchianico, S., Möller, L., Odnevall Wallinder, I., Elihn, K., Karlsson, H.L., 2016. Nickel Release, ROS Generation and Toxicity of Ni and NiO Micro- and Nanoparticles. PLOS ONE 11, e0159684.

Lemaitre, B., Miguel-Aliaga, I., 2013. The digestive tract of Drosophila melanogaster. Annual review of genetics 47, 377-404.

Leso, V., Fontana, L., Mauriello, M.C., Iavicoli, I., 2017. Occupational Risk Assessment of Engineered Nanomaterials: Limits, Challenges and Opportunities.

Libralato, G., Galdiero, E., Falanga, A., Carotenuto, R., de Alteriis, E., Guida, M., 2017. Toxicity Effects of Functionalized Quantum Dots, Gold and Polystyrene Nanoparticles on Target Aquatic Biological Models: A Review. Molecules (Basel, Switzerland) 22.

Lin, C.M., Lu, T.Y., 2012. C60 fullerene derivatized nanoparticles and their application to therapeutics. Recent patents on nanotechnology 6, 105-113.

Liu, K., Liu, P.-c., Liu, R., Wu, X., 2015. Dual AO/EB Staining to Detect Apoptosis in Osteosarcoma Cells Compared with Flow Cytometry. Medical Science Monitor Basic Research 21, 15-20.

Liu, Y., Zhao, Y., Sun, B., Chen, C., 2013. Understanding the toxicity of carbon nanotubes. Accounts of chemical research 46, 702-713.

Loberg, J., Perez Holmberg, J., Mattisson, I., Arvidsson, A., Ahlberg, E., 2013. Electronic Properties of Nanoparticles Films and the Effect on Apatite-Forming Ability. International Journal of Dentistry 2013, 14.

Loos, C., Syrovets, T., Musyanovych, A., Mailander, V., Landfester, K., Nienhaus, G.U., Simmet, T., 2014. Functionalized polystyrene nanoparticles as a platform for studying bio-nano interactions. Beilstein J Nanotechnol 5, 2403-2412.

Ma, P., Luo, Q., Chen, J., Gan, Y., Du, J., Ding, S., Xi, Z., Yang, X., 2012. Intraperitoneal injection of magnetic Fe(3)O(4)-nanoparticle induces hepatic and renal tissue injury via oxidative stress in mice. International journal of nanomedicine 7, 4809-4818.

Magaye, R., Zhao, J., Bowman, L., Ding, M., 2012. Genotoxicity and carcinogenicity of cobalt-, nickel- and copper-based nanoparticles. Experimental and therapeutic medicine 4, 551-561.

Markus, M.A., Napp, J., Behnke, T., Mitkovski, M., Monecke, S., Dullin, C., Kilfeather, S., Dressel, R., Resch-Genger, U., Alves, F., 2015. Tracking of Inhaled Near-Infrared Fluorescent Nanoparticles in Lungs of SKH-1 Mice with Allergic Airway Inflammation. ACS Nano 9, 11642-11657.

Martel, J., Young, J.D.-E., 2008. Purported nanobacteria in human blood as calcium carbonate nanoparticles. Proceedings of the National Academy of Sciences 105, 5549-5554.

Mashock, M.J., Zanon, T., Kappell, A.D., Petrella, L.N., Andersen, E.C., Hristova, K.R., 2016. Copper Oxide Nanoparticles Impact Several Toxicological Endpoints and Cause Neurodegeneration in Caenorhabditis elegans. PLoS One 11, e0167613.

Massarsky, A., Abraham, R., Nguyen, K.C., Rippstein, P., Tayabali, A.F., Trudeau, V.L., Moon, T.W., 2014. Nanosilver cytotoxicity in rainbow trout (Oncorhynchus mykiss) erythrocytes and hepatocytes. Comp Biochem Phys C 159.

Mazel, C.H., 1997. Coral fluorescence characteristics: excitation/emmission spectra, fluorescence efficiences, and contribution to apparent reflectance, Ocean Optics XIII. SPIE, p. 6.

McConnell, L.H., Fink, J.N., Schlueter, D.P., M. G. Schmidt, J.R., 1973. Asthma Caused by Nickel Sensitivity. Annals of Internal Medicine 78, 888.

McLaughlin, J.M., Bratu, D.P., 2015. Drosophila melanogaster Oogenesis: An Overview. Methods in molecular biology (Clifton, N.J.) 1328, 1-20.

McWilliams, A., 2014. Global Markets for Nanocomposites, Nanoparticles, Nanoclays, and Nanotubes.

Medina, S.H., El-Sayed, M.E., 2009. Dendrimers as carriers for delivery of chemotherapeutic agents. Chem Rev 109, 3141-3157.

Mintzer, M.A., Grinstaff, M.W., 2011. Biomedical applications of dendrimers: a tutorial. Chemical Society reviews 40, 173-190.

Mishra, V., Baranwal, V., Mishra, R.K., Sharma, S., Paul, B., Pandey, A.C., 2016. Titanium dioxide nanoparticles augment allergic airway inflammation and Socs3 expression via NF-kappaB pathway in murine model of asthma. Biomaterials 92, 90-102.

Mittal, a.k., Chisti, Y., Banerjee, U., 2013. Synthesis of metallic nanoparticles using plant extracts.

Mody, V.V., Siwale, R., Singh, A., Mody, H.R., 2010. Introduction to metallic nanoparticles. Journal of Pharmacy and Bioallied Sciences 2, 282-289.

Mohamed, H.E.A., Sone, B.T., Fuku, X.G., Dhlamini, M.S., Maaza, M., 2018. Green synthesis of BiVO4 nanorods via aqueous extracts of Callistemon viminalis. AIP Conference Proceedings 1962, 040004.

Morimoto, Y., Hirohashi, M., Ogami, A., Oyabu, T., Myojo, T., Hashiba, M., Mizuguchi, Y., Kambara, T., Lee, B.W., Kuroda, E., Tanaka, I., 2012. Expression of cytokine-induced neutrophil chemoattractant in rat lungs following an intratracheal instillation of micron-sized nickel oxide nanoparticle agglomerates. Toxicology and Industrial Health 30, 851-860.

Morozov, Y.G., Belousova, O.V., Kuznetsov, M.V., 2011. Preparation of nickel nanoparticles for catalytic applications. Inorganic Materials 47, 36-40.

Muhlfeld, C., Geiser, M., Kapp, N., Gehr, P., Rothen-Rutishauser, B., 2007. Re-evaluation of pulmonary titanium dioxide nanoparticle distribution using the "relative

deposition index": Evidence for clearance through microvasculature. Particle and fibre toxicology 4, 7.

Mukherjee, P., Bhattacharya, R., Wang, P., Wang, L., Basu, S., Nagy, J.A., Atala, A., Mukhopadhyay, D., Soker, S., 2005. Antiangiogenic properties of gold nanoparticles. Clinical cancer research : an official journal of the American Association for Cancer Research 11, 3530-3534.

Mulfinger, L., Solomon, S.D., Bahadory, M., Jeyarajasingam, A.V., Rutkowsky, S.A., Boritz, C., 2007. Synthesis and Study of Silver Nanoparticles. Journal of Chemical Education 84, 322.

Murray, A.R., Kisin, E., Inman, A., Young, S.H., Muhammed, M., Burks, T., Uheida, A., Tkach, A., Waltz, M., Castranova, V., Fadeel, B., Kagan, V.E., Riviere, J.E., Monteiro-Riviere, N., Shvedova, A.A., 2013. Oxidative stress and dermal toxicity of iron oxide nanoparticles in vitro. Cell biochemistry and biophysics 67, 461-476.

Nanotechnologies., T.P.o.E., 2015. Consumer Products Inventory.

Ni, M., Leung, M.K.H., Leung, D.Y.C., Sumathy, K., 2007. A review and recent developments in photocatalytic water-splitting using TiO2 for hydrogen production. Renewable and Sustainable Energy Reviews 11, 401-425.

Nunes, A.C., Majkrzak, C.F., Berkowitz, A.E., 1983. Polarized neutron study of the magnetization density distribution within a CoFe2O4 colloidal particle. Journal of Magnetism and Magnetic Materials Journal of Magnetism and Magnetic Materials 39, 59-63.

O'Brien, R.W., Midmore, B.R., Lamb, A., Hunter, R.J., 1990. Electroacoustic Studies of Moderately Concentrated Colloidal Suspensions. Faraday discussions of the Chemical Society., 301.

Oberdörster, G., Ferin, J., Finkelstein, G., Wade, P., Corson, N., 1990. Increased pulmonary toxicity of ultrafine particles? II. Lung lavage studies. Journal of Aerosol Science 21, 384-387.

Oberdörster, G., Maynard, A., Donaldson, K., Castranova, V., Fitzpatrick, J., Ausman, K., Carter, J., Karn, B., Kreyling, W., Lai, D., Olin, S., Monteiro-Riviere, N., Warheit, D., Yang, H., 2005. Principles for characterizing the potential human health effects from exposure to nanomaterials: elements of a screening strategy. Particle and fibre toxicology 2, 8.

Oberdorster, G., Oberdorster, E., Oberdorster, J., 2005. Nanotoxicology: an emerging discipline evolving from studies of ultrafine particles. Environ Health Perspect 113, 823-839.

Olcott, M.H., Henkels, M.D., Rosen, K.L., L.Walker, F., Sneh, B., Loper, J.E., Taylor, B.J., 2010. Lethality and Developmental Delay in Drosophila melanogaster Larvae after Ingestion of Selected Pseudomonas fluorescens Strains. PLOS ONE 5, e12504.

Olszta, M.J., Cheng, X., Jee, S.S., Kumar, R., Kim, Y.-Y., Kaufman, M.J., Douglas, E.P., Gower, L.B., 2007. Bone structure and formation: A new perspective. Materials Science and Engineering: R: Reports 58, 77-116.

Onuma, K., Sato, Y., Ogawara, S., Shirasawa, N., Kobayashi, M., Yoshitake, J., Yoshimura, T., Iigo, M., Fujii, J., Okada, F., 2009. Nano-scaled particles of titanium dioxide convert benign mouse fibrosarcoma cells into aggressive tumor cells. The American journal of pathology 175, 2171-2183.

Pan, Y., Wu, Q., Qin, L., Cai, J., Du, B., 2014. Gold nanoparticles inhibit VEGF165-induced migration and tube formation of endothelial cells via the Akt pathway. BioMed research international 2014, 418624.

Pandey, U.B., Nichols, C.D., 2011. Human disease models in Drosophila melanogaster and the role of the fly in therapeutic drug discovery. Pharmacological reviews 63, 411-436.

Pang, H., Lu, Q., Li, Y., Gao, F., 2009. Facile synthesis of nickel oxide nanotubes and their antibacterial, electrochemical and magnetic properties. Chemical communications (Cambridge, England), 7542-7544.

Pappus, S.A., Mishra, M., 2018. A Drosophila Model to Decipher the Toxicity of Nanoparticles Taken Through Oral Routes. Advances in experimental medicine and biology 1048, 311-322.

Pareek, V., Bhargava, A., Gupta, R., Jain, N., Panwar, J., 2017. Synthesis and Applications of Noble Metal Nanoparticles: A Review.

Park, E.-J., Yi, J., Chung, K.-H., Ryu, D.-Y., Choi, J., Park, K., 2008. Oxidative stress and apoptosis induced by titanium dioxide nanoparticles in cultured BEAS-2B cells. Toxicology Letters 180, 222-229.

Park, M.V., Neigh, A.M., Vermeulen, J.P., Fonteyne, L.J., Verharen, H.W., Briedé, J.J., Loveren, H., Jong, W.H., 2011. The effect of particle size on the cytotoxicity, inflammation, developmental toxicity and genotoxicity of silver nanoparticles. Biomat 32.

Peng, Q., Huo, D., Li, H., Zhang, B., Li, Y., Liang, A., Wang, H., Yu, Q., Li, M., 2018. ROS-independent toxicity of Fe3O4 nanoparticles to yeast cells: Involvement of mitochondrial dysfunction. Chemico-biological interactions 287, 20-26.

Petersen, E.J., Henry, T.B., 2012. Methodological considerations for testing the ecotoxicity of carbon nanotubes and fullerenes: review. Environmental toxicology and chemistry 31, 60-72.

Philbrook, N.A., Winn, L.M., Afrooz, A.R., Saleh, N.B., Walker, V.K., 2011. The effect of TiO(2) and Ag nanoparticles on reproduction and development of Drosophila melanogaster and CD-1 mice. Toxicology and applied pharmacology 257, 429-436.

Phillips, J.I., Green, F.Y., Davies, J.C.A., Murray, J., 2010. Pulmonary and systemic toxicity following exposure to nickel nanoparticles. American Journal of Industrial Medicine 53, 763-n/a.

Piao, M.J., Kang, K.A., Lee, I.K., Kim, H.S., Kim, S., Choi, J.Y., Choi, J., Hyun, J.W., 2011. Silver nanoparticles induce oxidative cell damage in human liver cells through inhibition of reduced glutathione and induction of mitochondria-involved apoptosis. Toxicol Lett 201, 92-100.

Piret, J.P., Vankoningsloo, S., Mejia, J., Noel, F., Boilan, E., Lambinon, F., Zouboulis, C.C., Masereel, B., Lucas, S., Saout, C., Toussaint, O., 2012. Differential toxicity of copper (II) oxide nanoparticles of similar hydrodynamic diameter on human differentiated intestinal Caco-2 cell monolayers is correlated in part to copper release and shape. Nanotoxicology 6, 789-803.

Pisanic, T.R., 2nd, Zhang, Y., Wang, T.H., 2014. Quantum dots in diagnostics and detection: principles and paradigms. Analyst 139, 2968-2981.

Prijic, S., Sersa, G., 2011. Magnetic nanoparticles as targeted delivery systems in oncology. Radiology and oncology 45, 1-16.

Rahman, M.F., Wang, J., Patterson, T.A., Saini, U.T., Robinson, B.L., Newport, G.D., Murdock, R.C., Schlager, J.J., Hussain, S.M., Ali, S.F., 2009. Expression of genes related to oxidative stress in the mouse brain after exposure to silver-25 nanoparticles. Toxicol Lett 187.

Raveendran, P., Fu, J., Wallen, S.L., 2003. Completely “Green” Synthesis and Stabilization of Metal Nanoparticles. Journal of the American Chemical Society 125, 13940-13941.

Robbins, M.A., 2013. The Collector’s Book of Fluorescent Minerals. Springer US.

Rodríguez, H., 2018. Nanotechnology and Risk Governance in the European Union: the Constitution of Safety in Highly Promoted and Contested Innovation Areas. Nanoethics NanoEthics : Studies of New and Emerging Technologies 12, 5-26.

Roh, J.Y., Eom, H.J., Choi, J., 2012. Involvement of caenohabditis elegans mapk signaling pathways in oxidative stress response induced by silver nanoparticles exposure. Toxicological Research 28, 19-24.

Saikia, J.P., Paul, S., Konwar, B.K., Samdarshi, S.K., 2010. Nickel oxide nanoparticles: A novel antioxidant. Colloids and Surfaces B: Biointerfaces 78, 146-148.

Sanpui, P., Chattopadhyay, A., Ghosh, S.S., 2011. Induction of apoptosis in cancer cells at low silver nanoparticle concentrations using chitosan nanocarrier. ACS Appl Mater Interfaces 3, 218-228.

Sayes, C.M., Reed, K.L., Warheit, D.B., 2011. Nanoparticle toxicology: measurements of pulmonary hazard effects following exposures to nanoparticles. Methods in molecular biology (Clifton, N.J.) 726, 313-324.

Schägger, H., 2006. Tricine-SDS-PAGE. Nature Protocols 1, 16-22.

Schaming, D., Remita, H., 2015. Nanotechnology: from the ancient time to nowadays.

Schlesinger, M.J., 1990. Heat shock proteins. The Journal of biological chemistry 265, 12111.

Schluesener, J.K., Schluesener, H.J., 2013. Nanosilver: application and novel aspects of toxicology. Archives of toxicology 87, 569-576.

Scown, T.M., Santos, E.M., Johnston, B.D., Gaiser, B., Baalousha, M., Mitov, S., Lead, J.R., Stone, V., Fernandes, T.F., Jepson, M., van Aerle, R., Tyler, C.R., 2010. Effects of aqueous exposure to silver nanoparticles of different sizes in rainbow trout. Toxicol Sci 115, 521-534.

Scuri, M., Chen, B.T., Castranova, V., Reynolds, J.S., Johnson, V.J., Samsell, L., Walton, C., Piedimonte, G., 2010. Effects of titanium dioxide nanoparticle exposure on neuroimmune responses in rat airways. Journal of toxicology and environmental health. Part A 73, 1353-1369.

Semenza, G.L., 1998. Hypoxia-inducible factor 1: master regulator of O< sub> 2</sub> homeostasis. Current opinion in genetics & development 8, 588-594.

Setyawati, M.I., Khoo, P.K., Eng, B.H., Xiong, S., Zhao, X., Das, G.K., Tan, T.T., Loo, J.S., Leong, D.T., Ng, K.W., 2013. Cytotoxic and genotoxic characterization of titanium dioxide, gadolinium oxide, and poly(lactic-co-glycolic acid) nanoparticles in human fibroblasts. Journal of biomedical materials research. Part A 101, 633-640.

Sharma, H.S., Hussain, S., Schlager, J., Ali, S.F., Sharma, A., 2010. Influence of nanoparticles on blood-brain barrier permeability and brain edema formation in rats. Acta neurochirurgica. Supplement 106, 359-364.

Shi, H., Magaye, R., Castranova, V., Zhao, J., 2013. Titanium dioxide nanoparticles: a review of current toxicological data. Particle and fibre toxicology 10, 15.

Shin, S.C., Kim, S.H., You, H., Kim, B., Kim, A.C., Lee, K.A., Yoon, J.H., Ryu, J.H., Lee, W.J., 2011. Drosophila microbiome modulates host developmental and metabolic homeostasis via insulin signaling. Science (New York, N.Y.) 334, 670-674.

Simon, M., Saez, G., Muggiolu, G., Lavenas, M., Le Trequesser, Q., Michelet, C., Deves, G., Barberet, P., Chevet, E., Dupuy, D., Delville, M.H., Seznec, H., 2017. In situ quantification of diverse titanium dioxide nanoparticles unveils selective endoplasmic reticulum stress-dependent toxicity. Nanotoxicology 11, 134-145.

Singh, S.R., Liu, W., Hou, S.X., 2007. The Adult Drosophila Malpighian Tubules Are Maintained by Pluripotent Stem Cells. Cell stem cell 1, 191-203.

Sondi, I., Salopek-Sondi, B., 2004. Silver nanoparticles as antimicrobial agent: a case study on E. coli as a model for Gram-negative bacteria. Journal of Colloid and Interface Science 275, 177-182.

Song, P., Wen, D.-s., Guo, Z.X., Korakianitis, T., 2008. Oxidation investigation of nickel nanoparticles.

Srnová-Šloufová, I., Vlčková, B., Bastl, Z., Hasslett, T.L., 2004. Bimetallic (Ag)Au Nanoparticles Prepared by the Seed Growth Method: Two-Dimensional Assembling, Characterization by Energy Dispersive X-ray Analysis, X-ray Photoelectron Spectroscopy, and Surface Enhanced Raman Spectroscopy, and Proposed Mechanism of Growth. Langmuir 20, 3407-3415.

Stapleton, P.A., McBride, C.R., Yi, J., Nurkiewicz, T.R., 2015. Uterine microvascular sensitivity to nanomaterial inhalation: An in vivo assessment. Toxicology and applied pharmacology 288, 420-428.

Stokes, D., Royal Microscopical, S., 2008. Principles and practice of variable pressure/environmental scanning electron microscopy (VP-ESEM).

Sukhanova, A., Bozrova, S., Sokolov, P., Berestovoy, M., Karaulov, A., Nabiev, I., 2018. Dependence of Nanoparticle Toxicity on Their Physical and Chemical Properties. Nanoscale Res Lett 13, 44.

Suzuki, B.Y., 2010. Insect Development: Morphogenesis, Molting and Metamorphosis. The Quarterly Review of Biology 85, 509-509.

Tedja, R., Lim, M., Amal, R., Marquis, C., 2012. Effects of serum adsorption on cellular uptake profile and consequent impact of titanium dioxide nanoparticles on human lung cell lines. ACS Nano 6, 4083-4093.

Tee, B.C.K., Wang, C., Allen, R., Bao, Z., 2012. An electrically and mechanically self-healing composite with pressure- and flexion-sensitive properties for electronic skin applications. Nature nanotechnology 7, 825.

Tong, H., Ma, W., Wang, L., Wan, P., Hu, J., Cao, L., 2004. Control over the crystal phase, shape, size and aggregation of calcium carbonate via a l-aspartic acid inducing process. Biomaterials 25, 3923-3929.

Tuli, H.S., Kashyap, D., Bedi, S.K., Kumar, P., Kumar, G., Sandhu, S.S., 2015. Molecular aspects of metal oxide nanoparticle (MO-NPs) mediated pharmacological effects. Life Sciences 143, 71-79.

van der Zande, M., Vandebriel, R.J., Van Doren, E., Kramer, E., Herrera Rivera, Z., Serrano-Rojero, C.S., Gremmer, E.R., Mast, J., Peters, R.J., Hollman, P.C., Hendriksen, P.J., Marvin, H.J., Peijnenburg, A.A., Bouwmeester, H., 2012. Distribution, elimination, and toxicity of silver nanoparticles and silver ions in rats after 28-day oral exposure. ACS Nano 6, 7427-7442.

Vance, M.E., Kuiken, T., Vejerano, E.P., McGinnis, S.P., Hochella, M.F., Jr., Rejeski, D., Hull, M.S., 2015. Nanotechnology in the real world: Redeveloping the nanomaterial consumer products inventory. Beilstein Journal of Nanotechnology 6, 1769-1780.

Veruscka, L., Luca, F., Maria Chiara, M., Ivo, I., 2017. Occupational Risk Assessment of Engineered Nanomaterials: Limits, Challenges and Opportunities. Current Nanoscience 13, 55-78.

Vidavsky, N., Addadi, S., Mahamid, J., Shimoni, E., Ben-Ezra, D., Shpigel, M., Weiner, S., Addadi, L., 2014. Initial stages of calcium uptake and mineral deposition in sea urchin embryos. Proceedings of the National Academy of Sciences 111, 39-44.

Volk, G.M., Goss, L.J., Franceschi, V.R., 2004. Calcium Channels are Involved in Calcium Oxalate Crystal Formation in Specialized Cells of Pistia stratiotes L. Annals of Botany 93, 741-753.

Wadhera, A., Fung, M., 2005. Systemic argyria associated with ingestion of colloidal silver. Dermatology online journal 11, 12.

Wang, Y, Xia, 2004. Bottom-Up and Top-Down Approaches to the Synthesis of Monodispersed Spherical Colloids of Low Melting-Point Metals. Nano Letters 4.

Wang, B., Chen, N., Wei, Y., Li, J., Sun, L., Wu, J., Huang, Q., Liu, C., Fan, C., Song, H., 2012. Akt signaling-associated metabolic effects of dietary gold nanoparticles in Drosophila. Scientific Reports 2, 563.

Wang, J., Zhou, G., Chen, C., Yu, H., Wang, T., Ma, Y., Jia, G., Gao, Y., Li, B., Sun, J., Li, Y., Jiao, F., Zhao, Y., Chai, Z., 2007. Acute toxicity and biodistribution of different sized titanium dioxide particles in mice after oral administration. Toxicol Lett 168, 176-185.

Wang, X., Fang, H., Huang, Z., Shang, W., Hou, T., Cheng, A., Cheng, H., 2013. Imaging ROS signaling in cells and animals. Journal of molecular medicine (Berlin, Germany) 91, 917-927.

Warheit, D.B., Webb, T.R., Reed, K.L., Frerichs, S., Sayes, C.M., 2007. Pulmonary toxicity study in rats with three forms of ultrafine-TiO2 particles: differential responses related to surface properties. Toxicology 230, 90-104.

Wen, L.-S., Santschi, P.H., Gill, G.A., Paternostro, C.L., Lehman, R.D., 1997. Colloidal and Particulate Silver in River and Estuarine Waters of Texas. Environmental science & technology 31, 723-731.

Wilson, C.L., Natarajan, V., Hayward, S.L., Khalimonchuk, O., Kidambi, S., 2015. Mitochondrial dysfunction and loss of glutamate uptake in primary astrocytes exposed to titanium dioxide nanoparticles. Nanoscale 7, 18477-18488.

Wolf, D.E., 2013. Fundamentals of fluorescence and fluorescence microscopy. Methods in cell biology 114, 69-97.

Wu, X., Liu, H., Liu, J., Haley, K.N., Treadway, J.A., Larson, J.P., Ge, N., Peale, F., Bruchez, M.P., 2003. Immunofluorescent labeling of cancer marker Her2 and other cellular targets with semiconductor quantum dots. Nature biotechnology 21, 41-46.

Wu, Z.G., Munoz, M., Montero, O., 2010. The synthesis of nickel nanoparticles by hydrazine reduction. Advanced Powder Technology 21, 165-168.

Yang, P.-H., Sun, X., Chiu, J.-F., Sun, H., He, Q.-Y., 2005. Transferrin-mediated gold nanoparticle cellular uptake. Bioconjugate chemistry 16, 494-496.

Yang, X., Gondikas, A.P., Marinakos, S.M., Auffan, M., Liu, J., Hsu-Kim, H., Meyer, J.N., 2012. Mechanism of silver nanoparticle toxicity is dependent on dissolved silver and surface coating in caenorhabditis elegans. Environmental Science and Technology 46, 1119-1127.

Yang, Y.X., Song, Z.M., Cheng, B., Xiang, K., Chen, X.X., Liu, J.H., Cao, A.N., Wang, Y.L., Liu, Y.F., Wang, H.F., 2014. Evaluation of the toxicity of food additive silica nanoparticles on gastrointestinal cells. Journal of Applied Toxicology 34, 424-435.

Yin, J.-J., Liu, J., Ehrenshaft, M., Roberts, J.E., Fu, P.P., Mason, R.P., Zhao, B., 2012. Phototoxicity of nano titanium dioxides in HaCaT keratinocytes—Generation of reactive oxygen species and cell damage. Toxicology and applied pharmacology 263, 81-88.

Yu, S.-j., Yin, Y.-g., Liu, J.-f., 2013. Silver nanoparticles in the environment. Environmental Science: Processes & Impacts 15, 78-92.

Zhang, L.W., Monteiro-Riviere, N.A., 2009. Mechanisms of quantum dot nanoparticle cellular uptake. Toxicological sciences : an official journal of the Society of Toxicology U6 - ctx_ver=Z39.88-2004&ctx_enc=info%3Aofi%2Fenc%3AUTF-8&rfr_id=info:sid/summon.serialssolutions.com&rft_val_fmt=info:ofi/fmt:kev:mtx:journal&rft.genre=article&rft.atitle=Mechanisms+of+quantum+dot+nanoparticle+cellular+uptake&rft.jtitle=Toxicological+sciences+%3A+an+official+journal+of+the+Society+of+Toxicology&rft.au=Zhang%2C+Leshuai+W&rft.au=Monteiro-Riviere%2C+Nancy+A&rft.date=2009-07-01&rft.eissn=1096-0929&rft.volume=110&rft.issue=1&rft.spage=138&rft_id=info:pmid/19414515&rft.externalDocID=19414515&paramdict=en-US U7 - Journal Article 110, 138.

Zhang, W.-x., 2003. Nanoscale Iron Particles for Environmental Remediation: An Overview. Journal of Nanoparticle Research 5, 323-332.